

ABSTRACT

BAKER, JORDAN LEE. Characterization and Fate of Ammonia from Poultry Operations: Their Emissions, Transport, and Deposition in the Chesapeake Bay. (Under the direction of Dr. Viney P. Aneja and Dr. S. Pal Arya).

Poultry operations on the Maryland Eastern Shore contribute to approximately 99% of the total agricultural ammonia/nitrogen livestock emissions on the Delmarva peninsula. Emissions from poultry operations lead to the deposition of ammonia/nitrogen to the Chesapeake Bay causing detrimental environmental impacts as a result. The goal of this study is to determine how much ammonia/nitrogen is being deposited to the Chesapeake Bay from poultry operations from the Maryland Eastern Shore. Ammonia observations were taken from 23 sites across Maryland's Eastern Shore to collect data for atmospheric transport and deposition model validation. Sussex County, Delaware and counties in Virginia were omitted from this study due to a lack of data availability. Based on the meteorology during the measurements, and using this data, a deposition velocity of 2.4 cm/s was selected via sensitivity analysis that is used to apply to an air quality model (AERMOD) simulation of 603 poultry facilities. Using AERMOD, a domain approximately 134 km by 230 km was simulated with a resolution of 2 km by 2 km to determine the fate of ammonia/nitrogen emitted from these poultry facilities. Emission factors from the U.S. Environmental Protection Agency in conjunction with Carnegie-Mellon University were used in the calculation of ammonia emission rate. Realistic terrain heights and meteorology observations were used by utilizing the data processing available with AERMOD, AERMAP and AERMET. A deposition velocity of 2.4 cm/s shows an overestimation of total deposition which is ~2 times the total emission. Therefore, a deposition velocity (0.15 cm/s) from similar studies are used to find total ammonia/nitrogen deposition. Using a deposition velocity of 0.15 cm/s, results from the AERMOD simulation show that approximately

$1,284 \pm 0.24$ tonnes ($1,415 \pm 0.22$ US tons) of nitrogen is deposited to both the Chesapeake Bay and the Delmarva peninsula landmass due to ammonia/nitrogen release from poultry AFOs. This is approximately 8.37% of the total emission from these facilities. Of the total deposition, about 397 ± 0.01 tonnes of ammonia/nitrogen is deposited directly to the Chesapeake Bay with the remaining 886.5 tonnes being deposited to the Delmarva peninsula. It is difficult, to accurately determine the indirect deposition to the Chesapeake Bay from poultry AFOs. Meteorological conditions and deposition velocity affect deposition at a given time and can produce dramatic increases and decreases depending on atmospheric moisture, stability, and temperature. A seasonal analysis was performed to find the season with the highest average ambient concentration and deposition. Results show that spring is the season with the most deposition while winter is the season with the lowest. Autumn is the season with the third highest deposition calculation and summer is the season with the second highest seasonal deposition. It is important to note that modeled concentrations and deposition fluxes are calculated assuming that the same rate of ammonia/nitrogen is being emitted at all times. It is determined that the majority of ammonia/nitrogen (and nitrogen associated) is being transported through waterways from the land mass to the Chesapeake Bay.

© Copyright 2018 by Jordan Baker

All Rights Reserved

Characterization and Fate of Ammonia from Poultry Operations: Their Emissions, Transport,
and Deposition in the Chesapeake Bay

by

Jordan Lee Baker

A thesis submitted to the Graduate Faculty of
North Carolina State University
in partial fulfillment of the
requirements for the degree of
Master of Science

Marine, Earth, & Atmospheric Sciences

Raleigh, North Carolina

2018

APPROVED BY:

Dr. Viney P. Aneja
Co-Chair of Advisory Committee

Dr. S. Pal Arya
Co-Chair of Advisory Committee

Dr. John T. Walker

DEDICATION

This thesis is dedicated to all those that have supported me along the way. It is incredible the impact that positive attitudes and supportive people can have on your life. Through many rough times there were tough and supportive conversations. In the good times, there were many people with which to share laughter and happiness. Thank you to my family, friends, and family of friends for all the love and support throughout these six years. A special thank you to the closest of these friends, the love of my life, Rebecca.

BIOGRAPHY

Jordan Lee Baker was born in Dunn, North Carolina on April 4, 1994 to Lisa Bass and Willie Baker Jr.. As a child, Jordan enjoyed sports, fishing, and helping on his grandfather's farm. Over many acres of farmland, summer thunderstorms could be seen in the distance with cumulonimbus clouds towering into the humid North Carolina sky. This would be the first of many years of fascination with weather and the science of meteorology. In 2012, Jordan graduated from Midway High School in his hometown of Dunn, North Carolina, with an intent to become a meteorologist. After completing his bachelor's degree in 2016 at North Carolina State University, Jordan was presented with an extraordinary opportunity to combine both his passion for meteorology and a new-found interest in air quality. In June of 2016, Jordan entered the Air Quality Research Group at North Carolina State University under the direction of Dr. Viney Aneja. During his master's project, Jordan was able to work closely with the Chesapeake Bay Foundation on ammonia/nitrogen emissions and deposition. Jordan was also able to work with Dr. S. Pal Arya and Dr. John T. Walker of the U.S. EPA. Upon completion of his degree in 2018, Jordan will be employed by the National Weather Service in Wilmington, North Carolina as a staff meteorologist to pursue a lifelong dream.

ACKNOWLEDGMENTS

This research was supported by the Chesapeake Bay Foundation. I would like to thank my committee members for their time, expertise, and assistance in preparing this thesis, Dr. Viney P. Aneja, Dr. S. Pal Arya, and Dr. John Walker. I would like to thank Dr. Wayne Robarge for resources, assistance, and preparation during the duration of the project's sampling campaign. I would also like to thank the members of the Air Quality Research Group, Dr. Bill Battye, Casey Bray, Pornpan "Lugwaa" Uttamang, Rebecca Wiegand, Alberth Nahas, Qi Li and Mike Pirhalla. I am thankful for the resources from the Maryland Department of the Environment and the Chesapeake Bay Foundation. The United States Department of Agriculture, United States Environmental Protection Agency, North Carolina State University's High Performance Computing Center, National Center for Climate Data, and Carnegie-Melon University were tremendous resources throughout this project. Finally, I would like to thank the members, employees, and volunteers of the Chesapeake Bay Foundation for their hospitality, cooperation, patience, and hard work during the entirety of this project.

TABLE OF CONTENTS

| | |
|--|-----|
| LIST OF TABLES | vi |
| LIST OF FIGURES | vii |
| LIST OF EQUATIONS..... | ix |
| Chapter 1: Introduction | 1 |
| 1.1. Background | 1 |
| 1.2. Emission Factors..... | 2 |
| 1.3. Fate of Atmospheric Ammonia/Nitrogen | 3 |
| 1.4. Previous Research..... | 7 |
| 1.4.1. Similar Studies | 7 |
| 1.4.2. Dispersion Modeling..... | 8 |
| 1.4.3. Deposition Velocities..... | 12 |
| Chapter 2: Methods | 15 |
| 2.1. Measurements | 15 |
| 2.2. Modeling Procedures | 16 |
| 2.2.1. Input Data Processing | 18 |
| 2.2.2. Single Facility | 19 |
| 2.2.3. Sensitivity Analysis | 20 |
| 2.2.4. Main Simulation..... | 21 |
| Chapter 3: Results..... | 22 |
| 3.1. Sampling Results | 22 |
| 3.2. Sensitivity Analysis Results..... | 23 |
| 3.3. Main Simulation Results..... | 25 |
| 3.3.1. Single Facility Results and Analysis..... | 25 |
| 3.3.2. Concentration Results and Analysis | 29 |
| 3.3.3. Deposition Results and Analysis | 30 |
| 3.3.4. Seasonal Results and Analysis | 32 |
| Chapter 4: Conclusions | 34 |
| References | 38 |
| Tables | 44 |
| Figures..... | 52 |
| Appendices..... | 71 |
| Appendix A | 72 |

LIST OF TABLES

| | | |
|---------|--|----|
| Table 1 | Estimated Emissions from CMU Emission Factors, USDA Activity Data for AFO/Commercial animal populations on the Delmarva Peninsula. | 44 |
| Table 2 | CMU Emission Factors broken down by emission factor contribution. Each total emission factor has three contributing sources of emission including confinement, storage, and land application. | 45 |
| Table 3 | A summary of measured deposition velocities for selected studies (located in the reference column). Deposition velocities based on studies in previous years. Site indicates the area in which the measurements were taken. | 46 |
| Table 4 | A summary of site characteristics describing nearby structures, trees, and potential ammonia/nitrogen sources. The description simply defines the site as either Residential, Rural, Commercial, or Marine. | 47 |
| Table 5 | A summary of sampled ammonia mass and concentrations for Trip 1 (September 8, 2017 – September 22, 2017) | 48 |
| Table 6 | A summary of sampled ammonia mass and concentrations for Trip 2 (September 22, 2017 – October 6, 2017). | 49 |
| Table 7 | Summary of precision of duplicate samplers at site 18. Concentrations are provided for both Trip 1 and Trip 2 in units of parts per billion (ppb). | 50 |
| Table 8 | Summary of precision of duplicate samplers at site 20. Concentrations are provided for both Trip 1 and Trip 2 in units of parts per billion (ppb). | 51 |

LIST OF FIGURES

| | | |
|-----------|--|----|
| Figure 1 | Breakdown of ammonia/nitrogen emissions from various source categories throughout the United States as of 2000 | 52 |
| Figure 2 | Map of Maryland, Delaware, and Virginia counties on the Chesapeake Bay included in animal population and emission factor calculation. Used as a reference for county-level emissions and calculation throughout the document. | 53 |
| Figure 3 | Outline diagram of a single ALPHA Sampler with its components listed..... | 54 |
| Figure 4 | ALPHA sampler support on a metal post. Picture of placement in the field. | 55 |
| Figure 5 | The extent of the model domain is covered by the borders of the edges of the figure. red locations are areas where samplers were placed. Their number is listed next to the sampler indicator. | 56 |
| Figure 6 | Sampler results shown with units of parts per billion of ammonia/nitrogen (ppb). Colors indicate relative strength of the concentration for Trip 1..... | 57 |
| Figure 7 | Sampler results shown with units of parts per billion of ammonia/nitrogen (ppb). Colors indicate relative strength of the concentration for Trip 2..... | 58 |
| Figure 8 | Mean Normalized Absolute Error (MNAE) with values of MNAE on the y-axis as it correlates with receptor on the x-axis. | 59 |
| Figure 9 | Normalized Mean Bias over all deposition velocities considered during the sensitivity analysis portion of the study. | 60 |
| Figure 10 | Comparison of modeled concentration against observed concentrations in the sensitivity analysis..... | 61 |
| Figure 11 | Wind rose for meteorology data used in all simulations associated with this study. The wind rose shows predominant wind speed and wind direction..... | 62 |
| Figure 12 | Total deposition of ammonia/nitrogen as a function of distance from a source. | 63 |
| Figure 13 | Average Annual Deposition Flux as a Function of Distance from an AFO Source..... | 64 |
| Figure 14 | Average ammonia/nitrogen concentration over the Delmarva Peninsula during the 2017 year..... | 65 |

| | |
|---|----|
| Figure 15 Annual total (dry + wet) deposition of ammonia/nitrogen. Units of the deposition are in grams per meter squared per year..... | 66 |
| Figure 16 Average ammonia/nitrogen concentration over the Delmarva Peninsula during the winter season..... | 67 |
| Figure 17 Average ammonia/nitrogen concentration over the Delmarva Peninsula during the spring season..... | 68 |
| Figure 18 Average ammonia/nitrogen concentration over the Delmarva Peninsula during the summer season..... | 69 |
| Figure 19 Average ammonia/nitrogen concentration over the Delmarva Peninsula during the fall season..... | 70 |

LIST OF EQUATIONS

| | |
|---|----|
| Equation 1 General form of the AERMOD Gaussian plume calculation within both the stable boundary layer (SBL) and the convective boundary layer (CBL) in terms of a bi-Gaussian probability density function. | 9 |
| Equation 2 Gaussian ground level concentration (GLC) equation for a continuous source with an initial source strength (Q_x)..... | 9 |
| Equation 3 AERMOD mass equation indicating change of the pollutant strength as a function of loss by dry deposition. | 10 |
| Equation 4 Dry deposition flux equation | 10 |
| Equation 5 Equation for the effective volume concentrations of an ALPHA passive sampler as a function of diffusivity, surface area, and exposure time. | 16 |
| Equation 6 Measured atmospheric ammonia concentration from the difference measured mass of a pollutant analyzed from a passive sampler and the measured mass of a pollutant analyzed from a travel blank | 16 |

Chapter 1. Introduction

1.1. Background

According to the U.S. Environmental Protection Agency's (EPA) Guidance for Federal Land Management in the Chesapeake Bay Watershed, agricultural activity (Figure 1) accounts for a large portion of the excess nitrogen and phosphorous causing an imbalance within the Chesapeake Bay (U.S. Environmental Protection Agency, 2010; Sheeder et al., 2002)). The U.S. EPA's total maximum daily load (TMDL) indicates that 44% of excess nitrogen and phosphorus deposited to the Bay is due to agricultural activity (U.S. Environmental Protection Agency, 2014). It is believed that within the Chesapeake Bay watershed, poultry operations account for two-thirds of the excess nitrogen and half of the excess phosphorous released from agricultural operations (National Research Council, 2003). Increased nitrogen and phosphorous to the Chesapeake Bay can lead to adverse environmental impacts, and mainly eutrophication from surface algal blooms (Linker et al., 2013; Gilbert et al., 2001; Aneja et al., 2001; Battye et al., 2017). Of the intensive agricultural production on the Delmarva peninsula, Table 1 shows that poultry contribute more than 99% of the total atmospheric ammonia/nitrogen emission on the Delmarva Peninsula from animal waste. The data in Table 1 shows ammonia/nitrogen emissions from counties on the Delmarva Peninsula. Since data is provided on a county level, emission factors are applied to activity data from the counties shown only in Figure 2.

To determine transport and deposition of emitted ammonia requires air quality modeling. Many processes act on emitted pollutants in the atmosphere and these processes are largely nonlinear. Energy exchanges at the surface influence planetary boundary height and turbulence leading to mass changes and momentum exchanges carrying the pollutant varying distances (Arya, 1999). Surface concentration modeling and deposition are analyzing impacts to sensitive

ecosystems such as the waterways. Few studies before have attempted to quantify the emissions from a small sector of the Chesapeake Bay watershed. Therefore, the objective of this study is to quantify the deposition of ammonia/nitrogen to the Chesapeake Bay and its surrounding bodies from only animal feeding operations (AFOs) located on the Maryland Eastern Shore (yellow region in Figure 2). Ammonia/nitrogen is chosen for this study because ammonia/nitrogen is one of the largest emissions from AFOs due to animal waste and the inability of animals to digest the existing nitrogen in feed, resulting in deposition of ammonia-nitrogen which may exacerbate the nitrogen load in the Bay (Bittman & Mikkelsen, 2009).

1.2. Emission Factors

Emission factors were developed by Carnegie-Mellon University (CMU) with assistance from the U.S. EPA (emission factors are referred to as EPA/CMU emission factors) are specific to the chemical species of ammonia/nitrogen. Each emission factor is broken into three categories that contribute to the total emission factor. Confinement refers to the emission from animal residing inside of a AFO and emission from the waste produced within the contained area. Storage refers to the emission of ammonia/nitrogen from the storage of the waste removed from the AFO. Land application, as implied, is the emission of ammonia/nitrogen after waste is applied to a field as fertilizer. The total emission factor is the sum of confinement, storage, and land application. It is difficult to report emission factors for specific farms and areas, but we assume that each farm uses no waste management control such as alum and that the farm stores and applies waste in the vicinity of the original confinement area. This allows us to apply the total emission factor for a single AFO. These values and the total for selected agricultural species are provided in Table 2. Emission factors from EPA/CMU are reported in units of kg NH₃ per animal per month. The total emission factor for poultry displayed and used in our study

is the addition of confinement, storage, and land application. The number is then extrapolated to kg NH₃ per animal per year as 0.200 kg NH₃ animal⁻¹ year⁻¹.

Previous research suggests that the emission factor can be as high as 0.789 kg NH₃ per bird per year (Gates et al., 2005). Others suggest the EPA/CMU emission factor is much higher than measurements which estimate an emission factor of approximately 0.035 kg NH₃ per bird per year (Burns et al., 2007). Given the high variability in animal population management practices, climate, and waste management control practices, our best estimate of an emission factor is to use U.S. EPA/CMU-suggested emission factors. There will be high variability in any one area, but the EPA/CMU emission factor should provide an overall average of emission factors for any management practice. This is important because the EPA/CMU model developed in 2004 is based on individual counties and waste management practices.

1.3. Fate of Atmospheric Ammonia/Nitrogen

At the Earth's surface, NH_x (= NH₃ + NH₄⁺) has a range of well understood, beneficial, and detrimental consequences for humans and the environment (Tomich et al., 2016; Battye et al., 2017). For example, nitrogen fertilizers have had a beneficial effect on agriculture globally by increasing crop yields. However, the high loading of reactive nitrogen (reactive nitrogen includes all biologically active, chemically reactive, and radiatively active nitrogen compounds in the atmosphere and biosphere of the earth, in contrast to non-reactive gaseous N₂) has led to deleterious effects on the environment, such as acidification of soils, forest decline, decreased visibility from increased aerosol production, and elevated nitrogen (both ammonia/nitrogen and oxides of nitrogen (NO_x)) concentrations in ground and surface waters, possibly leading to enhanced eutrophication in downwind ecosystems (Asman, 1998; Aneja et al., 1998; Krupa, 2003; Baek and Aneja 2004; Schlossberg, 2017). Thus, there is a need to study the NH_x

deposition changes, spatial distribution, and transport of ammonia/nitrogen from agricultural sources (both crop and animal) to gain a better understanding of effective means to control or reduce excess amounts of ammonia/nitrogen and ammonium deposition.

The fate of atmospheric ammonia/nitrogen depends on nearby moisture, vegetation, emission strength, temperature, wind velocity and other atmospheric species present. One of the more well-understood mechanisms for the removal of atmospheric ammonia/nitrogen is in-cloud and below-cloud scavenging. During the process of in-cloud scavenging, ammonia/nitrogen within the cloud can interact with cloud condensation nuclei (CCN). Gaseous ammonia/nitrogen interacts with the liquid on the surface of CCN and is transformed into a dissolved gas; effectively removing the available atmospheric ammonia/nitrogen by diluting the gas to low levels (Jitra et al., 2015). Below-cloud scavenging is a similar process in which the ammonia/nitrogen does not reach equilibrium with the raindrop before the drop begins descending to Earth during precipitation. As the rain drop falls, ammonia/nitrogen is taken in by the raindrop and dissociation begins as in in-cloud scavenging, however, in this process the ammonia/nitrogen being scavenged is at a much lower atmospheric level, below the lifting condensation level (LCL) (Seinfeld & Pandis, 2016). Ammonia/nitrogen's high solubility and effective Henry's Law constant make these processes much easier for the species to be removed, as compared to other atmospheric gases (Seinfeld & Pandis, 2016). Any atmospheric ammonia/nitrogen that is not dry deposited or scavenged by raindrops is converted into atmospheric ammonium (Seinfeld & Pandis, 2016). This is done through the interaction of gaseous ammonia/nitrogen with small water particles not large enough to effectively dissolve gaseous ammonia/nitrogen. The conversion of ammonia/nitrogen to atmospheric ammonium is important because the ammonium aerosol has a much longer lifetime than ammonia/nitrogen and

is an alkaline species that is readily used in the process of PM_{2.5} formation, especially in the presence of sulfuric acid and nitric acid (Jacobson, 1999).

Dry deposition is another process which is important to understand the fate of atmospheric ammonia/nitrogen. Depending on an area's temperature, humidity, and precipitation, dry deposition may be the largest contributor to nitrogen deposition from ammonia/nitrogen releases (Duyzer, 1994). Dry deposition refers to the removal of atmospheric gases or particles without the presence of moisture in the atmosphere. Given that ammonia/nitrogen is highly soluble, it is important to consider dry deposition to both vegetation and to water bodies. Water bodies in which ammonia/nitrogen is deposited can cause dissolution of ammonia/nitrogen and lead to an additional nitrogen deposition mechanism (Larsen et al., 2001). With no natural surface resistance due to the solubility of the species, ammonia/nitrogen uptake by water bodies is efficient and is an important factor in areas where wetlands, rivers, lakes, or other large ocean bodies are present (Larsen et al., 2001). This fact coupled with the concentration of emission sources on the Delmarva Peninsula makes dry deposition a vital topic of this study.

The dry deposition flux (equation 4), F_d ($\mu\text{g}/\text{m}^2/\text{s}$), is calculated as the product of the concentration, $C(x,y,z)$ ($\mu\text{g}/\text{m}^3$), and a deposition velocity, V_d (cm/s), computed at a reference height, z_r (m). The dry deposition flux is calculated on an hourly basis and summed to obtain the total flux for the user-specified period based on a user-defined land use type which is described as one of nine categories. AERMOD allows users to select either urban land with no vegetation (1), agricultural land (2), rangeland (3), forest (4), suburban areas with mainly grassy areas (5), suburban areas with mainly forested land (6), bodies of water (7), barren land (desert) (8), and non-forested wetland (9) land-use types.

Dry deposition to areas with vegetation is important for ground water transport of nitrogen as well. Deposition of ammonia/nitrogen to vegetation is more complicated with respect to water bodies because the framework of the resistance model is introduced. When calculating or observing deposition to vegetation, atmospheric gases have several factors influencing their deposition fluxes. These deposition fluxes are aerodynamic resistance, quasi-laminar resistance, and surface resistance. Aerodynamic resistance is the resistance of gases to transport from the atmosphere to the surface and is denoted as r_a . Once a gas molecule makes it to the surface for exchange, it must overcome a differentially turbulent layer that relies on molecular diffusion and surface (canopy) characteristics. Quasi-laminar resistance is denoted as r_b . The surface resistance (r_c) is determined by the surface to which the gas is depositing. There are separate resistances that make up the surface resistance which include water resistance, ground resistance, and foliar resistance. Typically, a vegetative canopy exists which involves additional complex resistances, but is usually referred to as the canopy resistance (Seinfeld & Pandis, 2016).

In addition to the resistance model, the bi-directional flux of ammonia/nitrogen needs to be considered. The bi-directional flux of ammonia/nitrogen suggests that when the stomatal compensation point of ammonia/nitrogen in the atmosphere is higher than the compensation point at the surface, ammonia/nitrogen will deposit to the surface of leaves whereas where the compensation point of the gas is higher at the leaf surface than in the atmosphere, the vegetation will emit ammonia/nitrogen (Pleim et al., 2013; Farquhar et al., 1980). In the scope of this study, this could imply that the emission area is much larger than previously thought. Large poultry facilities and high concentrations of ammonia/nitrogen will lead to transport of ammonia/nitrogen away from the facility as ammonia emitted from waste is ventilated from the

AFO to the environment. This is done, primarily, by exhaust fans located on the end of the housing facility and windows/doors on the end and along the side of the structure. Other factors such as ammonia/nitrogen diffusivity, temperature, moisture and stability will limit or exacerbate the transport distances away from poultry facilities (Arya, 1999).

1.4. Previous Research

1.4.1. Similar Studies

This study builds off of an initial research project conducted on the Delmarva peninsula in 2004 by Siefert et al. (2013). Siefert et al. uses inverse modeling to determine the emission strength of the initial poultry operation, while the model used in this study infers the original strength of the emission source from Maryland AFO population data and emission factors from CMU/EPA. Previous studies such as O'Shaughnessy and Altmaier (2011) have used inverse modeling in this way with the American Meteorological Society (AMS)/United States Environmental Protection Agency (EPA) Regulatory Model (AERMOD). Reports interested in the improvement of computer modeling such as the Airsheds and Watersheds III: A Shared Resources Workshop in November of 2000 note that emissions at the source are most important in improving computer model performance. Inverse modeling is a way to do this, and while this study does not seek to improve emission data, it does attempt to validate samplers with regional deposition and concentration data, unlike many previous studies. The objective of this study is to assume the initial strength with emission factors from the US EPA/CMU and simulate the concentration and deposition at a point downwind and later in time. Unfortunately, due to the differences in emission strength, Siefert et al. (2013) and this study are too different to be compared.

Overall, few studies have attempted to apply AERMOD to a regional scale simulation. In addition to this, little has been done with AERMOD regarding atmospheric ammonia/nitrogen. Many applications associated with AERMOD are hydrogen sulfide emissions and dispersion of these pollutants in the vicinity of industrial practices both agricultural and manufacturing (O'Shaughnessy and Altmaier, 2011; Khoirunissa 2018). Sutton et al. (1998) conducted a study utilizing AERMOD's dispersion calculations in the United Kingdom (U. K.) to model ammonia/nitrogen in a rural landscape, locally. This study found that AERMOD shows accuracy despite no inclusion of the bi-directional flux and land-cover data which would influence the transport distances. Again, this study was performed locally and does not comment on AERMOD's ability on a regional level.

It is also important to keep in mind that the assumption of this study is that no waste management practice is used throughout the modeling domain and that the facilities are producing at maximum capacity at all times throughout the duration of the simulation. This will provide an upper-limit scenario for nitrogen deposition and concentration values. Limitations within this study limit the ability of the model to create temporal variations in emissions and no activity and sale data are available from the farms themselves.

1.4.2. Dispersion Modeling

AERMOD is a dispersion model currently supported by the US EPA. It is similar to other dispersion models in that they are designed to model the transport of certain chemicals. Initially, the US Military began to experiment with dispersion modeling due to fear of chemical weapons (U.S. Environmental Protection Agency, 2013). This led to scientists becoming aware of atmospheric dispersion and the first theories regarding atmospheric pollutant transport were developed by Taylor in 1922. Vertical dispersion was later investigated and led to the Gaussian

plume dispersion equation that is the base of Gaussian plume models used today, including AERMOD (Arya, 1999).

AERMOD uses steady-state plume modeling to calculate concentrations and depositions with the goal being to limit large errors in model output based on small changes from input parameters (U.S. Environmental Protection Agency, 2013). The horizontal and vertical concentration distribution is assumed to be Gaussian in the stable boundary layer (SBL) and unlike many dispersion models, it is assumed to be a bi-Gaussian probability density function following statistical concentration distributions in the convective boundary layer (CBL) (Deardorf & Willis, 1985; Briggs, 1993). The general form of AERMOD within both the SBL and the CBL is:

$$C(x, y, z) = \frac{Q}{u} P_y(y, x) P_z(z, x) \quad (1)$$

With C being the average concentration, Q being emission strength, u being average wind speed, and P_y and P_z being the probability density function describing the concentration as a statistical expression away from the model centerline (Peters, 2015). Divisions occur between the convective boundary layer and the transition between the two. However, most time is spent in the CBL due to surface energy budgets and final concentrations, before several forms of dispersion equations describe plume dispersion, lateral dispersion, and natural centerline fade dispersion (U.S. Environmental Protection Agency, 2013). While concentration calculations are forefront of the AERMOD formulation, deposition is the most important parameter discussed in this study. Chamberlain (1953) describes the simple deposition model used in AERMOD's formulation involving calculations of ground-level concentrations (GLC) with a continuous source:

$$C_0(x, y, 0) = \frac{Q_x}{\pi \sigma_y \sigma_z u} \exp\left(-\frac{y^2}{2\sigma_y^2}\right) \exp\left(-\frac{H^2}{2\sigma_z^2}\right) \quad (2)$$

where Q_x is the depleted source strength downwind at a distance of x and governed by the mass equation:

$$\frac{\partial Q_x}{\partial x} = - \int_{-\infty}^{\infty} F_d(x, y) \, dy \quad (3)$$

And the dry deposition flux:

$$F_d(x, y, 0) = v_d C(x, y, 0) \quad (4)$$

This is termed as a source-depletion model and is a linear relationship allowing deposition to be calculated from GLC calculations with previous determination of SBL contributions and CBL contributions within AERMOD calculations and a prescribed deposition velocity (v_d) (Cimorelli et al., 2005).

Several studies in the past have used AERMOD's dispersion capabilities. Many studies have modeled H₂S emissions and dispersion using AERMOD. Khoirunissa 2018 used AERMOD to find H₂S emissions within geothermal emissions from power plants in Indonesia. AERMOD proved to perform well during long simulations and within 3 km of the source (Khoirunissa, 2018). Other studies have used AERMOD to inverse model emission factors for better representation of emission from agricultural practices. O'Shaughnessy and Altmaier, 2011 found that AERMOD worked effectively when using inverse modeling, especially at distances of less than 6 km. Other studies have used AERMOD at local scales, but no literature search during this review found AERMOD-related studies that incorporated areas larger than 50 km.

Attempting to apply AERMOD to a regional application rather than a local application makes this study unique. Other studies have successfully applied AERMOD to a local application of ammonia. Bajwa et al. (2008) used AERMOD to determine deposition velocities under different seasons and stability conditions. Deposition velocities were modeled on a local scale and found that total deposition occurred within 2,500 m of the source. Thoebald et al. (2012) compared

AERMOD, Atmospheric Dispersion Modelling System (ADS), Local Atmospheric Dispersion and Deposition (LADD), and the Operational Priority Substances model (OPS-st) in terms of concentration within 1,000 m of a source. Input processes were varied throughout the study which found that for area and volume sources, AERMOD and OPS-st predicted larger concentration which hold for a case study involving such studies. Overall AERMOD, ADS, and OPS-st performed well as compared to an acceptability criteria. Hanna et al. (2001) compared ADMS, AERMOD, and ISC3 at downwind distances of 10 to 20 km. A total of 6 sites were used in the comparison. AERMOD shows better performance at 3 of these 6 sites over ADMS and ISC3. Hall et al. (2000) compared AERMOD, ADMS, and ISC in terms of local dispersion over complex terrain. While no complex terrain exists in the work that follows, it is important to note that AERMOD's dispersion calculations are one of many possibilities based on the model formulation, and that AERMOD, due to its advanced dispersion processes and advanced meteorological preprocessor (AERMET), shows good performance at local scales.

Since AERMOD requires raw METAR data as meteorological input into the model, sources of atmospheric data are limited to National Weather Service ASOS stations. Combined with the fact that meteorological conditions can vary substantially across a domain of 50 km, particularly when that domain covers a large water body and a coastal climate, some areas of the modeling domain will not be simulated using accurate meteorology. However, this does not mean that the simulated data are not accurate. Since the regional weather pattern is captured in the model, the simulation from AERMOD will give a general idea of the atmospheric conditions at all modeling receptors.

1.4.3. Deposition Velocities

Schrader and Brummer (2014) have reviewed published deposition velocities for various land use types and found annual mean values ranging from 0.1 to 1.8 for semi-natural, 0.4 to 3.0 for mixes forests, and 0.2 to 7.1 for agricultural sites. Deposition velocities span more than an order of magnitude within and across land use types. Phillips et al. (2004) conducted their study in an area similar to the Maryland Eastern Shore. Phillips et al. (2004) is listed as a semi-natural site and is downwind of the North Carolina State University Research Farm in central North Carolina. Measurements were not taken at the facility, but were taken downwind over turf grass. We did not take direct measurements at a CAFO, but several samplers were located downwind (~ 5km) of large facilities and in open grass fields. Table 3 summarizes the findings of ammonia deposition velocities from several studies.

In general, semi-natural sites have a relatively low deposition velocity with many ranging from about 0.6 – 1.8 centimeters per second (Bajwa et al., 2008; Benedict et al., 2013; Kirchner et al., 2005; Myles et al., 2011). This varies based on area of study and time of year. Most studies report deposition velocities during the fall season with some reporting annual means for comparison (Bajwa et al., 2008; Phillips et al., 2004; Neirynck et al., 2005; Neirynck et al., 2007; Myles et al., 2011). Phillips measured a deposition velocity of 2.8 cm/s during the daytime during the fall. Phillips et al. is an outlier when considering all of the semi-natural studies due to its proximity to farm operations near North Carolina State University. Some studies were conducted in areas of mixed forests. Surprisingly, these show very high deposition velocities. In mixed forest biomes, Neirynck et al. conducted two separate studies in similar regions in 2005 and 2007. Deposition velocities were reported as 3.5 cm/s during the day in the summer and 2.4 cm/s during the night in the summer, in 2005. A similar study conducted in 2007 found a

deposition velocity of only 2.8 cm/s during the day in the summer. This speaks to the high variability that is seen when measuring deposition velocity of ammonia/nitrogen even in the same region. Stability, ground temperature, moisture, and other factors may limit or amplify deposition velocities.

The final area of interest in the literature review is involved with agricultural soils. In areas downwind of agricultural production, deposition velocities are expected to be lower than any other type of land types considered unless the measurements are taken downwind of the ammonia source or in areas of fertilized soils. This is reflected in a study done by Myles et al. (2011) who reports a deposition velocity at 7.1 cm/s over a fertilized soil. Other studies such as Baek et al. (2006) finds a deposition velocity of 6.3 cm/s within the downwind fetch of the ammonia source. Studies with deposition velocities below 1 cm/s are likely located within a few hundred to 1,000 m of an ammonia source or in soils with a high ammonia concentration (Bajwa et al., 2008). Theobald et al. (2012) found a deposition velocity of 0.15 cm/s in a study that compares local transport of ammonia within 1 km of a source using different dispersion models. Pleim et al. (2013) does provide some reasoning for this with more in-depth analysis provided by Cooter et al. (2010) for agricultural soils specifically. The ammonia/nitrogen bi-directional flux can cause areas of low deposition velocities near ammonia/nitrogen sources. High concentrations tend to increase the surface resistance which will decrease the effective dry deposition velocity and decrease the overall deposition to an area. Therefore, a constant deposition velocity may not capture the extent of ammonia transport near areas of high concentration such as downwind of intensive animal operations. This difference can be as high as a factor of 10 at the source and a factor of 2, 60 m downwind of the source (Jones et al., 2007). This would also explain why semi-natural and mixed forests have a higher deposition

velocity. Furthermore, it would be an additional benefit to include variable deposition velocities based on land-use categories. Within the model formulation, the user is allowed to define land-use characteristics in relation to the source. With a large quantity of modeled sources and unknown land-use characteristics of each individual site, the land-use is assumed for the entirety of the region. Defining land-use at each site individually will improve the quality of modeled transport and provide more detailed surface characteristics that are used in the model output calculation.

Chapter 2. Methods

2.1. Measurements

The CEH ALPHA sampler (Figure 3) is a passive sampler for measuring NH₃ in air. The sampler uses a phosphorous acid coated filter, which serves to capture the ammonia/nitrogen for later analysis. A white PTFE (Teflon) membrane protects the filter whilst allowing gaseous ammonia/nitrogen to diffuse through for capture. The membrane is positioned facing downwards during sampling. This prevents rainfall from adversely impacting the measurements. The membrane end of the sampler is sealed with a protective cap whilst not being exposed. The passive sampling system consists of replicate ALPHA samplers attached to a shelter on a pole or post at about 2.0 m above ground, which for our situation, is approximately 6.5 feet (Figure 4). Replicate samplers are used in order to give a more reliable estimation of the air concentration of ammonia/nitrogen. All samplers are transported in sealed plastic containers for protection.

Phosphorous acid is suitable as an absorbent for temperate climates and is used to coat the ALPHA membranes for all samplers during this measurement campaign. Phosphorous acid is prepared prior to the day of use, but as close to the day of setup as possible. The phosphorous acid coating solution is 50 mL with 52.0 grams of phosphorous acid dissolved in 100 mL of deionized water to create the solution. Laboratory preparation of the coated filters continues with an 8-step process as the solution will be applied to the filter paper. Step 1 involves the transfer of the coating solution to a small capped bottle. Next, approximately 10 filters at a time are arranged on clean petri dishes. Working as quickly as possible, 40 mL of solution is applied to the center of each filter. After this, the petri dishes containing the filters are placed inside a desiccator. Next, a vacuum pump is connected to the desiccator until each filter appears visibly dry after about 3 minutes. The coated filters are then ready to be stored until deployment. CEH

recommends that, for storage, each filter is stored inside of a small petri dish that is sealed and placed inside grip-seal bags and then stored in an airtight container.

In addition to the monitors, 10 travel blanks and laboratory blanks (8 during trip 1, and 6 during trip 2) were used during each trip for a total of 20 travel blanks and 14 laboratory blanks. Samplers were analyzed after each trip. Unfortunately, 2 travel blanks were discarded during trip 2 due to handling errors in the field. The analysis of the samplers is a straightforward process recommended by the supplier of the samplers. Analysis is done with the assumptions under Fick's Law which states that the diffusion path length is the distance from the mouth of the sampler to the reaction surface at the end of the tube which can be shortened by disturbances such as through the effect of turbulence. The total measured concentration is a function of this diffusion path length (L , m), the diffusivity of a pollutant (D ; for $\text{NH}_3 = 2.09 \times 10^{-5} \text{ m}^2 \text{ s}^{-1}$ at 10°C), and the area of the sampler's measuring surface (A , m^2).

$$V = \frac{DAt}{L} (\text{m}^{-3}) \quad (5)$$

From equation 5, the effective volume of the sampler is determined, and the final concentration (χ) is calculated based on the mass of the pollutant (m_e , μg) minus the mass of pollutant found to be in the travel/laboratory blanks (m_b , μg).

$$\chi = \frac{(m_e - m_b)}{V} (\mu\text{g m}^{-3}) \quad (6)$$

2.2. Modeling Procedures

AERMOD had a distinct advantage over other dispersion models such as CMAQ and ISC3. The CMAQ model does not allow for local scale calculation of concentrations and deposition. CMAQ is required for 3D calculation in as small as ~ 1 km horizontal spatial resolution which requires a tremendous amount of computing power. The inclusion of WRF meteorology leads to an additional increase in processing time and resources. Additionally,

WRF-generated meteorology introduces the possibility of further error in the model which is difficult to quantify (Appel et al., 2014). Using AERMOD allows us to increase the spatial resolution to as fine as 10 m, which is unprecedented in most air quality models. Additionally, we are able to use real-world meteorological data with AERMOD which reduces model error and increases the confidence in the model.

Limitations are introduced with AERMOD due to the spatial availability of meteorological data. Since there is only one meteorological station in our model, this station is used for the entire Maryland Eastern Shore along with Delmarva Virginia and southwestern Delaware and is maintained by the National Weather Service (NWS). From this station, wind speed, wind direction, temperature, dew point, and pressure are used to define surface parameters for use within AERMOD. Additional limitations of AERMOD include a lack of 3D calculations. Ground level concentrations and deposition are the only calculations available within AERMOD outputs. Having information on concentrations at a level just above ground-level would give us a more complete picture of ammonia/nitrogen scavenging and particulate matter (PM) formation, however, to an extent, wet deposition will give us the amount of ammonia/nitrogen converted to ammonium and used in PM formation (Walker et al., 2000). Another source of limitation would be land-use data. AERMOD does not allow us to distinguish areas of wetland, water, agricultural land, urban areas, and deciduous forest in a deposition post-calculation at individual receptors. This can be done at each source in radial directions, but since the land type at each source location is unknown, the model is forced to view the entire domain as continuous agricultural land. The density of this vegetation is determined by the seasonal classification defined by the user. This seasonal classification is simply an assignment of 1 of 5 categories to each of the 12 months. Classification 1, 2, 3, 4 and 5, are summer (lush), autumn (unharvested)

crops), late autumn (harvested crops, frost, and sparse vegetation), winter (continuous snow cover), and transitional spring (partially green coverage). Elevation data < 0 m gives the user information regarding areas of water. This limits our ability to calculate direct deposition to tributaries, water bodies, and wetlands and thus, calculated deposition in this study will be conservative.

2.2.1. Input Data Processing

AERMOD provides a terrain pre-processor created by the US EPA for AERMOD called AERMAP. This terrain preprocessor provides information for each receptor and source defined by UTM coordinates in the input file. Elevation data is extracted from the United States Geological Service (USGS) and the National Elevation Dataset. Within the terrain preprocessor, AERMAP calculates both elevation and flagged elevations to conform to hill heights for terrain that could cause issues within the main AERMOD simulation.

AERMOD also allows the user to process meteorology data from a single site in a program called AERMET. This is a limitation in several capacities. AERMOD does not allow the user to input multiple meteorology sources, which causes issues for covering a large domain. Localized meteorological effects such as sea-land breeze will not be calculated within the pre-processor. These are important mesoscale meteorological features that could have a localized effect on certain coastal locations. Despite this limitation, synoptic scale weather patterns will certainly be captured by the model and are perhaps the most important meteorological feature for non-coastal locations which is where most of the sources reside. AERMET requires raw METAR files which limits the selection of locations to those with automated ASOS/AWOS stations. Upper air data is obtained from the nearest site located on Wallops Island in Accomack Co., Virginia.

Emission rates from each AFO are determined using an appropriate emission factor for broilers as determined by CMU/EPA emission factors. Table 2 provides the breakdown into confinement, storage, and land application components of the total emission factor. The emission factor reported is an average over the lifetime of the activity type. As the bird ages and grows larger, the bird emits more ammonia. Conversely, chicks in their early growth stages emit very little. An average emission factor applied to a full broiler facility continuously for a year is a major assumption in this project. Using AFO population (activity) data from the USDA and facility specifications from the Maryland Department of the Environment (MDE), an emission rate for a ground-level area source ($\text{g m}^{-2} \text{ s}^{-1}$) is calculated. Once this emission rate is calculated and applied to the model, AERMOD calculates deposition based on the initial parameters of the ground-level source. Emissions are constant throughout the entire modeling period with no temporal variation. It is possible to vary the emissions based on time, but no data regarding housing or “clean-out” periods was provided by MDE.

2.2.2. Single Facility

To better understand the deposition distances experienced on a local scale, a “single-facility” simulation was performed. The goal of this analysis is to quantify how far deposition can occur over a single year from a single facility’s emissions. The facility selected for this study is a large facility with 14 houses and a flock capacity of 530,000 birds and it is assumed to be at full capacity year-round. The emission factor is listed in Table 2. The modeling domain is set with the center of the facility as the center of the domain. On each side of the facility, receptors are programmed to extend 5,000 m east, 5,000 m west, 5,000 m north, and 5,000 m south with a resolution of 100 m. Meteorology data from Salisbury, Maryland, during the year of 2017 is used as in the main simulation, described below. The single facility is treated as three

sources and are defined as source clusters: east (containing 5 houses), central (containing 4 houses), and west (containing 5 houses). Google Earth is used to find the angle at which the houses are positioned for realistic simulations.

2.2.3. Sensitivity Analysis

Deposition velocities are manually input into the model and varied from 1.0 cm/s to 4.0 cm/s to cover the range of possible deposition velocities in this study that would produce similar concentrations to the samplers. This also takes into account our land-use category and soil type. Concentration and deposition are output from the model. For the sensitivity analysis, we are primarily concerned with concentration data and its comparison to a total sampler concentration which is found by combining both periods of concentration data. The model is only run for 28 days during the sensitivity analysis and 365 days during the full-year deposition analysis. The deposition analysis is done after finding an appropriate deposition velocity for the model which is included in the results below.

Two comparison statistics were used in this study by reference from Irwin et al. (2013), Yu et al. (2006), and Zhang et al. (2006). The first statistic used for evaluation is Mean Normalized Absolute Error (MNAE) and the second statistic used for evaluation was a simple Normalized Mean Bias (NMB) which is suggested by most scientists in evaluation of observed versus predicted values in model evaluation. MNAE is a good metric for predictive and forecasting when involved in model metrics. This along with NMB can be a good predictor of simulated values against measured values (Irwin, 2013). One negative trait with MNAE is that it is normalized based on the observed value so this changes based on the measured value and makes it hard to compare between the error of each record (Yu et al., 2006). Additionally, NMB

can be positive or negative which will more clearly indicate if there was an over- or under-prediction of the model.

2.2.4. Main Simulation

The main simulation is set to cover the domain with an extent of 134 km by 230 km. Figure 5 shows this domain in full. Initial resolution was set to 1 km x 1 km, however computational demands were too high, so a final resolution of 2 km x 2 km was used. In addition to the high computational demands, post-processing files were on the order of 100s of gigabytes and this made opening and analyzing the files challenging. A total of 603 AFOs were modeled using Maryland AFO data provided by the Maryland Department of the Environment and collected in a format for analysis by Chesapeake Bay Foundation. As in the single facility, AFOs are assumed to be at full-capacity year-round.

Concentration is computed within the AERMOD program using the Gaussian plume equations and parameterizations of deposition. Deposition is calculated in two separate ways. Dry deposition is calculated using dry deposition velocities analyzed from the sensitivity analysis. Wet deposition is calculated using the Henry's Law Constant and diffusivity of air determined by previous studies and those recommended by EPA in their regulatory user's guide for AERMOD (Sander et al., 2015; Wesley et al., 2002). This will introduce a notable amount of error as the solubility of ammonia/nitrogen will vary temporally based on meteorological conditions and land-use.

Chapter 3. Results

3.1. Sampling Results

Unlike model simulations, samplers were deployed in two periods. The results were combined for model concentrations and are presented in Figure 6 and 7 as two separate periods. During the first period, ammonia concentration values ranged from 0.66 ppb to 4.75 ppb. Table 5 shows that spatial variability was high during the first trip with an average of 1.63 ppb and a standard deviation of 1.22 ppb. This is believed to be due to localized sources over which we had no control. Samplers 10-22 were placed in suburban/urban areas with high population density. This will cause variations in sampled concentrations as an increase in sources due to the application of fertilizer to lawns and additional sources of nitrogen from pets. Some marine and biogenic sources could be causing these high values as well. Samplers 1-7 were located in more remote areas, but these were also close to the coast. Meteorological factors such as sea breeze circulations, marine clouds, marine fog, and lower temperatures made areas near the coast and water bodies non-representative of a heavy agricultural area in terms of observed ammonia/nitrogen concentration. While all of these samplers give a good representation of the environment on a localized scale, sampler 8 and sampler 9 were placed in an area of high broiler population density (Figure 5). This leads us to believe that the results from these samplers will serve as the best litmus test in our sensitivity analysis due to the fact that the main source of measurable atmospheric ammonia is due primarily to the nearby broiler AFOs. During trip 2, sampler 8 and sampler 9 had similar results with an observed ammonia concentration of 1.44 and 1.26 ppb, respectively. Spatial variability continued, but decreased, during the second interval measurement period with a mean sampler concentration of 1.37 ppb with a standard deviation of 0.32 ppb (table 6). Table 7 and 8 present the precision of samplers placed in the same area to

give confidence to the measurements. Precipitation and stronger wind speeds led to lower concentrations as a tighter pressure gradient developed due to a tropical system that progressed just offshore. Precipitation also increased as moisture associated with the system was advected into the area. High solubility of ammonia leads to scavenging of ammonia from the environment in the presence of precipitation or activated cloud condensation nuclei (CCN) leading to lower concentrations. Despite this, sampler 8 and 9, again, showed similar concentrations of 1.65 and 1.63 ppb, respectively.

3.2. Sensitivity Analysis Results

Results of the sensitivity analysis are broken down into two statistical approaches, mean normalized absolute error (MNAE) (in Figure 8) and normalized mean bias (NMB) (in Figure 9). Figure 10 provides a visual representation of the relationship between modeled and observed concentrations when the sensitivity analysis is prescribed a deposition velocity of 1.0, 2.2, 2.4, and 2.6 cm s^{-1} . When looking at only the data points for sampler 8 and sampler 9, a deposition velocity of 2.4 cm/s shows that measured concentrations have a near 1:1 correlation with modeled concentrations. This area is indicated by a blue box in Figure 10. The remaining 20 sites do not reside on the 1:1 line. This pattern paradox may be explained because the sites located along the coast are upwind (during the measurement period) of the broiler AFOs of interest (Figure 11). With a predominant wind direction from the southwest, the source of ammonia concentration at these sites is from the Chesapeake Bay and mainland Virginia. Samplers at these sites will not capture the influence of broiler AFOs. However, these sites will represent the region's baseline ammonia concentration. Sampler 8 and 9 are the only 2 sites that will capture the influence of ammonia concentrations from broiler AFOs. A more appropriate location for sampling locations would be in Sussex County, Delaware (Figure 2) if a future

sampling campaign was desired. A plot of mean normalized absolute error is shown in Figure 8 and represents the lack of accuracy in samplers other than sampler 8 and sampler 9. This is likely due to the variability of localized sources in the region that are not included in the model and the influence of predominant wind direction, discussed above. The second statistic to be employed in the analysis of modeled concentrations is normalized mean bias. Figure 9 shows these results for each deposition velocity from 1.0 cm/s to 4.0 cm/s as suggested by a literature review of deposition velocities for semi-natural sites. For this metric, sampler 8 and sampler 9 were the only samplers considered. As one would expect, low deposition velocities lead to a large overprediction in modeled concentrations. A low deposition velocity leads to less deposition and higher ground level concentrations (GLC). Alternatively, high deposition velocities lead to an underprediction of GLC as more deposition occurs. A NMB of ~0 is seen for both a deposition velocity of 2.4 cm/s and 2.5 cm/s. A deposition velocity of 2.4 cm/s has a slightly lower NMB and is supported by Phillips et al. (2004) listed in the introduction of this study. MNAE also agrees with this conclusion.

We explored the use of a lower deposition velocity when the initial results using a deposition velocity of 2.4 cm/s indicated that total deposition within the model domain was greater than total emissions from the sources within the domain. From a mass balance standpoint, this result indicates that the model as parameterized with a deposition velocity of 2.4 cm/s is depositing NH₃ too rapidly. The result is inconsistent with literature which indicates that 10% or less of emitted NH₃ is deposited locally (500m – 1km) within the vicinity of animal production facilities (Walker et al., 2008; Fowler et al., 1998) and 15% or less of emissions deposition within a typical 12km x 12km model grid containing emissions from multiple animal production facilities (Dennis et al., 2010). The deposition velocity of 0.15 cm/s was chosen

because it reflects the lower end of the measured deposition velocities found in the literature (Schrader and Brummer et al., 2014), and therefore provides a lower end estimate of deposition to contrast with the deposition velocity of 2.4 cm/s, which likely represents the upper end. The lower deposition velocity of 0.15 cm/s is also more consistent with deposition velocities measured over agricultural land (median = 0.4 cm/s, Schrader and Brummer et al., 2014), which covers a large portion of the model domain. A deposition velocity of 2.4 cm/s would be more typical of coniferous forests, which are also found within the AERMOD model Domain. Finally, the deposition velocity of 0.15 cm/s has specifically been used in dispersion modeling of NH₃ deposition in the vicinity of animal production facilities (Theobald et al., 2012). As a final note, ignoring bias in other aspects of the model, a comparison of 0.15 cm/s versus 2.4 cm/s likely brackets the range of deposition rates across the land use types found in the model domain.

3.3. Main Simulation Results

3.3.1. Single Facility Results and Analysis

Annual averages were taken for a single facility in central Maryland Eastern Shore using a modeled deposition velocity of 2.4 cm/s. For this single facility, multiple attributes were investigated to better understand deposition, concentration, and seasonality of atmospheric ammonia/nitrogen. The main area of investigation is deposition distances from the poultry facility. It is important to note that within this study, a deposition velocity of 2.4 cm/s is used as it performs well for a concentration sensitivity analysis. The facility selected for this study was a very large facility and may not be representative of all poultry AFOs on the Delmarva Peninsula. Results show that for the average meteorological conditions on the Maryland Eastern Shore, and a deposition velocity of 2.4 cm/s, homes and businesses within 2.50 km of the source (in this case, a poultry AFO) will experience ammonia/nitrogen concentrations of 13.23 $\mu\text{g m}^{-3}$ (19.0

ppb). Under certain conditions, the concentration can be much higher and above the threshold for human detection (which is approximately 5,000 ppb) of ammonia/nitrogen. While this has no known health effects, it is a significant nuisance for communities near poultry AFOs (National Research Council, 2003). Concentrations quickly decline from this value to below 1.0 ppb beyond 2.50 km in either direction away from the source facility. No receptors within 3 km of the source facility in either direction showed concentrations above 0.039 ppb.

Seasonality was also investigated in regards to concentration. Concentrations were higher during the winter season due to AERMOD's calculation of the PBL and steady emission rate. Higher concentrations led to a larger area affected by impactful ammonia/nitrogen concentration. During the winter season, the area affected by concentrations above 40 ppb extended 800 m west, 700 m south, 1,200 m north, and 1,200 m east. This area is approximately 3.80 square km. The spring, summer, and fall season shows very little variation from the annual average. Without variable emission rates, this result is expected when meteorological factors are the only consideration, but during the summer, poultry will produce more waste due to heat stress and energy usage (Redwine et al., 2002). This will increase the available ammonia/nitrogen for emission. This is not reflected in the model since variable emission rates are difficult to accurately model and no available data exists to precisely model an AFO's residence time.

Approximately 91.4% of total deposition was found to occur within 2,000 m of an AFO source. This is a large proportion of the total deposition associated with a single AFO facility. Based on a deposition velocity of 2.4 cm/s, this is approximately 181% of the total emissions. Bajwa et al. (2008) found on average that approximately 9% of the total emissions from the source is deposited within 2,500 m of the source. Figure 13 gives a summary of transport

distances as represented by annual average deposition flux to the surface while Figure 12 shows the total deposition of ammonia/nitrogen as a function of distance from the source. Deposition fluxes decrease exponentially from the source as described by the Gaussian plume equation relating concentration and deposition described above in equations (2) and (4). This is an expected result and a function of the model formulation. It is important to note that the model does not incorporate the ammonia bi-directional flux. The highest amount of deposition occurred at 300 m from the source where concentrations were at their highest. This is corroborated by Theobald et al. (2012) which found that concentrations will decrease to $1 \text{ } \mu\text{g m}^{-3}$ or less at 1,000 m from a ground-level area source but will be at their maximum at distances of 300 m or more from the source.

Total deposition within the single facility simulation was found to be 181% of the total emissions. This result should not be possible when considering only sources from broiler AFOs because this implies that additional mass was created in the atmosphere or near the ground. However, according to the model formulation, available concentration is subject to deposition at a rate of the deposition velocity. Since the sensitivity analysis found such a large deposition velocity, even low concentration plumes are readily deposited. The reason for such a large deposition velocity found in the sensitivity analysis is due to sampler placement and the associated meteorology. Samplers located along the Bay measured a concentration not due to the influence of broiler AFOs. Sampler 8 and 9 did receive the ammonia concentration influence of broiler AFOs but also reported a concentration that only a deposition velocity of 2.4 cm/s could replicate. It would be a subject of future work to find a deposition velocity using a sensitivity analysis based on more sampler locations that felt the influence of broiler AFOs.

Because a deposition velocity of 2.4 cm/s leads to more total deposition than what is emitted, a deposition velocity more appropriate for the region, soil type, and model is used in the main simulation. Previous studies of ammonia deposition using AERMOD show low deposition velocities are favorable for total deposition calculations. A deposition velocity of 0.15 cm/s was used in the Theobald et al. (2012) work. This will likely lead to higher concentrations downwind and less total deposition than is found in this study. Downwind transport leads to an accumulation of maximum deposition distance of 300–500 m from a source. Only 8.5% of ammonia/nitrogen deposits at greater than 2,000 m. Dennis et al. (2010) used the Community Multi-scale Air Quality Model (CMAQ) to analyze transport distances of ammonia from CAFOs on a regional level. The study finds that a single 12 kilometer grid cell can have an influence up to 180 to 380 km from the source depending on the dry deposition formulation used. While this study contains multiple CAFOs, it also finds that 8-15% of the total emissions from a cluster of CAFO facilities deposits within the local grid cell. This means that up to 15% of a CAFO's emission will deposit within 12 km of the source. Given that local deposition is a linear function of local ground-level concentration, deposition velocity in which deposition will equal emissions was found to be approximately around 1.4 cm/s. This implies that a deposition below 1.4 cm/s must be used to find the appropriate fractional deposition which agrees with previous studies. The majority of emitted ammonia/nitrogen is turbulently diffused to negligible concentrations within the environment and some is scavenged by clouds or precipitation or chemically converted to particulate matter (PM) (Seinfeld & Pandis, 2016). Additional support to the application of a lower deposition velocity is based on the literature regarding measured deposition velocities. Over agricultural soils, a lower deposition velocity is found to be more appropriate. Given that other studies such as Hayashi et al. (2012), Katata et al. (2013), Benedict

et al. (2013), and Bajwa et al. (2008) have found that deposition velocities in agricultural soils is on the order of 0.1-1.0, a deposition velocity of 0.15 cm/s is realistic and justified.

3.3.2. Concentration Results and Analysis

Concentration results for a deposition velocity of 0.15 cm/s show an average ammonia/nitrogen concentration of $1.40 \mu\text{g m}^{-3}$ across the entire modeling domain. As Figure 14 shows, this is mostly over the Eastern Shore with a minimum in concentration over the Chesapeake Bay. Figure 14 and Figures 16-19 provide concentration data which will be directly proportional to deposition data due to the linear relationship between deposition flux and concentration when prescribed a constant deposition velocity. Figures 16-19 are seasonal deposition plots that show similar data during various seasons. With low ammonia compensation points on the surface of the water and high resistances of r_a , r_b , and r_c , the amount of ammonia/nitrogen reaching the Bay waters is likely higher than previously thought and is also depositing to the landmass or near other inland water bodies and subsequently feeding into the Chesapeake Bay. Unfortunately, determining the deposition to rivers, streams, and tributaries would be very difficult without land-use satellite data. Furthermore, understanding how this ammonia/nitrogen is transported within the transporting body itself is a separate issue as it is not advised to assume that all the nitrogen from ammonia/nitrogen is ultimately deposited within the Chesapeake Bay (Nus & Kenna, 2012). Additionally, meteorological factors such as land-sea breeze would limit transport to the Bay in general. Winds will blow perpendicular to the shore during the day where temperature gradients between the land and the water are appropriate (a common condition met in the area, but not measured in meteorology used in AERMOD simulations). This would protect Bay waters during appropriate atmospheric conditions. Winds

from the southwest will enhance this push away from the Bay waters as strong southwesterly winds advect ammonia concentrations toward southwestern Delaware (Figure 11).

3.3.3. Deposition Results and Analysis

AERMOD reports average deposition fluxes for each receptor within the modeling domain. Using a deposition velocity of 0.15 cm/s, Figure 15 provides annual average deposition flux (including both dry and wet deposition) over the course of a single year from AFOs on the Maryland Eastern Shore. Deposition fluxes are calculated hourly and averaged over the entirety of the modeling period and reported as an average deposition flux. A single deposition flux covers an area equal to the size of the model's resolution of 2 km by 2 km. Multiplying this area by the given deposition flux, which is expressed in units of grams per meter squared, will provide an estimate of the total deposition at a single point. The sum of this is the total deposition to the modeling domain. Average deposition fluxes show that throughout the year with meteorological observations and a deposition velocity of 0.15 cm/s, deposition over the modeling domain is calculated to be approximately 1,284 tonnes (1,415 US tons). From only 603 modeled sources, this is approximately 2.13 tonnes per AFO facility per year. Overall emissions totaled to 15,345 tonnes (16,914 US tons). Of the emitted ammonia/nitrogen, 8.37% deposited back to the domain. Sensitivity analysis based on using a deposition velocity of 2.4 cm/s, the fractional deposition was calculated as 181% (~27,774 tonnes per year). Previous studies found this conclusion to be unreasonable. Walker et al. (2008) found that about 10% of the emitted ammonia from a swine production facility deposited to the surface within about 500 m of the source. This fractional deposition at 2,500 m from the source peaked at around 13.5% of the total emissions. Fowler et al. (1998) found that about 3-10% of the locally emitted ammonia will deposit back locally. Additionally, Dennis et al. (2010) found that a fractional

deposition of around 8-15% of total emissions will occur within 12 km of a source facility.

Additionally, Shen et al. (2016) conducted a deposition study related to dairy farms and found that approximately 8.1% of the emitted ammonia/nitrogen is deposited within 1 kilometer from a source area (single dairy facility).

Linker et al. (2013) conducted a study to estimate the total nitrogen delivered to the Chesapeake Bay based on various CMAQ scenarios. The deposition of nitrogen was subdivided into regions that feed into the Chesapeake Bay watershed. According to Linker et al. (2013), the total nitrogen delivered to the Bay from all sources is approximately 13.5 million kilograms of nitrogen (N) per year from the Maryland Eastern Shore, including the Delaware watershed. Assuming that all of the deposition within the model is deposited to the watershed and eventually transports/deposits to the Bay, AERMOD calculates 1.06 million kilograms of N per year from broiler operations on the Maryland Eastern Shore alone. It is important to note that Linker et al. (2013) includes all known N sources as well as sources from the Chesapeake Bay watershed of Delaware.

Further analysis will provide estimates of deposition to both the land and the Chesapeake Bay waters. This is done with average deposition rates rather than maximum deposition rates. Over the Chesapeake Bay, total deposition is approximately 397 tonnes (438 US tons) according to the AERMOD simulation where elevations were at or below 0 m. Total deposition to the Maryland Eastern Shore is reported as 1,284 tonnes (1,415 US tons). This indicates that about 31% of the total deposition that occurs within the domain is depositing to the Chesapeake Bay waters directly. Moreover, this has not accounted for the additional input from indirect deposition to rivers, streams, and groundwater which will likely transport to the Chesapeake Bay. It is important to note that all houses are assumed to be at capacity year-round with constant

emissions. Emission factors also introduce error into the model as emission factors can vary based on waste management practice, weather, and poultry growth state. It is also assumed that no emission reduction material is used to mitigate reactive nitrogen emissions such as aluminum sulfate.

Meteorological effects will have a significant impact on the deposition (both wet and dry) over the domain. The most critical of these meteorological parameters affecting atmospheric dispersion and deposition is wind speed, wind direction, and stability (Arya, 1999). Figure 11 shows the wind direction and speed for the meteorology used in the main simulation. A predominant wind from the southwest is seen approximately 6% of the time. This will transport ammonia away from the bay and cause higher concentrations to exist over the terrestrial surface northeast of the concentration of sources. The second most common wind speed is from the south east. This wind speed again transports ammonia to the terrestrial body. High stability in the evening will tend to increase concentrations at the surface and lead to more deposition at this time of day. Unstable conditions will allow the plume to disperse effectively and lead to low concentrations.

3.3.4. Seasonal Results and Analysis

It is important to determine what season, if any, ammonia/nitrogen is deposited at a higher rate than other seasons (using a deposition velocity of 0.15 cm/s). Understanding this shows preferential meteorological conditions in which ammonia/nitrogen deposits. AERMOD calculated deposition flux linearly with concentration using equation 4 however, depletion rates do limit deposition. Spring recorded the highest deposition total with a total of 366.6 tonnes (404.1 US tons) of emitted ammonia/nitrogen. This is likely due to the combination of stable boundary layers in the early part of the season along with convective mixing associated with

high planetary boundary layer (PBL) heights later in the season, increasing turbulence near the ground associated with higher wind speeds, and a low moisture content during the late morning and afternoon early in the season. Additional precipitation during the spring also allows for an increase in wet deposition. Precipitation is also a sink of ammonia/nitrogen during the rainout and washout process (Seinfeld & Pandis, 2016). During the summer, deposition was also high with values reported at 319.7 tonnes (352.4 US tons). Summer boundary layers increase in height and increase transport distances and during the evening, boundary layers will trap pollutants near the surface, limit dispersion, and increase deposition in areas of high concentration. Unlike late spring and summer, winter temperatures will be lower and associated diffusion will be lower limiting transport distances of pollutants. The autumn season recorded the third-highest deposition value with 308.7 tonnes (340.3 US tons). Finally, the winter season was found to have the lowest deposition at 289.2 tonnes (318.8 US tons) of ammonia/nitrogen. During the summer, real-world deposition rates will increase due to an increase in emission rates, but this is a limitation with an emission factor approach and a modeled uniform emission rate. Temporal emissions are not included in this analysis. Under the assumptions of this study, the houses are at full capacity year-round and emission rates will be static. However, during the summer, animals consume more food and water leading to a higher emission of animal waste. Again, this is not accounted for in the model.

Chapter 4. Conclusions

This analysis is a combination of measurement and modeling. AERMOD has been proven to be accurate in predicting concentrations when prescribing a deposition velocity to the model and validating with meteorology and sampling results. However, when applying AERMOD to a regional scale, its abilities decrease as large deposition velocities have shown to give more deposition than is emitted from defined sources. Therefore, AERMOD's deposition capability decreases when applied to a regional scale. Differences in modeled concentration and observed concentrations were on average around $\pm 50\%$ for samplers located large distances from the source regions. AERMOD's ability to predict concentration drastically improved when considering sampled concentrations near the center of the source cluster. Figure 8 shows the mean bias applied to only samplers 8 and 9 and reports mean bias near 0. This is a promising result when applying the model to localized areas. Significantly higher mean biases in samplers at large distances from the source region are likely due to localized sources and the location of samplers being upwind of the largest cluster of broiler AFOs.

Direct annual deposition to the Chesapeake Bay is estimated to be around 397 tonnes (438 US tons). This is about 30% of deposited ammonia/nitrogen from the Maryland Eastern Shore. However, it is known that AERMOD is unable to calculate mesoscale meteorological features without being provided with appropriate weather data. Location of weather data used for this study was limited to areas in the center of the peninsula. In areas near the coast, sea breezes and other weather features of the marine environment will likely affect deposition calculations to the Bay. During the daytime, winds blowing inland will likely limit deposition to the Bay, but some conditions such as marine instabilities during the fall and early winter could exist to significantly increase deposition to the Bay surface. From this study, it is clear that

direct deposition of ammonia/nitrogen to the Chesapeake Bay is less than indirect deposition to rivers and tributaries within the watershed.

A single facility analysis was performed using a deposition velocity of 2.4 cm/s; which was determined from a sensitivity analysis of measured concentrations in an attempt to determine transport distances of ammonia/nitrogen from broiler AFOs. It was discovered that ammonia/nitrogen deposits approximately 91.4% within 2,000 m of the source. The fractional deposition with respect to emissions was approximately 181% which is much larger than expected. The reason for this overestimation is that a high deposition velocity determined from the sensitivity analysis was used to replicate concentrations at only 2 samplers. Because unfavorable meteorology (wind direction/marine-influenced stability) provided background results at 21 of the 23 sites, the deposition velocity was appropriate locally for the site at sampler 8 and 9, but the deposition velocity was unrepresentative of the region. This issue was resolved by using a deposition velocity (0.15 cm/s) based on previous studies which were applied either in modeling practices or measured.

When using a deposition velocity of 0.15 cm/s, indirect deposition due only to broiler AFOs to the Chesapeake Bay remains unknown. However, total deposition to the modeling domain is estimated to be around 1,284 tonnes (1,415 US tons). Of the emitted ammonia/nitrogen, 8.37% deposited back to the domain (using a deposition velocity of 0.15 cm/s). This is an appropriate percentage of the total emission and fits with previous studies. With nearly 70% of the modeled deposition settling to the landmass, indirect deposition will clearly provide the largest proportion of deposition to the Chesapeake Bay from river transport. Unfortunately, AERMOD does not allow users to get a specific land-use data set to be used in the analysis phase of the output. Additionally, vegetation is an important consideration of this

study. Dense forests will likely limit direct deposition to the Bay by taking up ammonia that would otherwise deposit to the water surface. These dense forests are near rivers and water bodies and may further limit deposition to the Chesapeake Bay.

From the analysis of seasonal deposition, it is determined that planetary boundary layer dynamics is the most important factor in determining modeled deposition flux along with wind speed and direction. This is true given an environment of similar emission rates and constant population in poultry AFO facilities. However, increased emission rates during the summer were not included in the AERMOD simulation and would be difficult to simulate given the current information on farm population and sales. With temporally varying emission rates, summer would be the season with the highest deposition rate which is similar to studies of swine production (Bajwa et al., 2008; James et al., 2012). With the current AERMOD simulation, increased PBL heights and turbulent flows from large surface energy fluxes result in higher concentrations and deposition fluxes during the summer.

Poultry AFOs were assumed to be at capacity during the duration of the model simulation. This is not a realistic approach, since it is difficult to model the temporal emissions from a single facility for 603 separate facilities. For future research, it is suggested that the simulation is run for a single growing cycle rather than an entire annual rotation. Additionally, seasonal variation is an important issue to address. Emission factors currently do not have a seasonal variation and it is important that the animal's metabolism be included in an emission factor or weighting of said emission factor. Regardless of whether realistic estimates of deposition to the Chesapeake Bay can be produced exactly in a model environment, an increase in emission will lead to an increase in deposition. Therefore, it is increasingly important to

understand the effects of ammonia/nitrogen-nitrogen deposition as the Chesapeake Bay area continues to grow and construct new sources of ammonia emission.

REFERENCES

- Aneja, V. P., G. C. Murray, and J. Southerland. (1998). Atmospheric nitrogen compounds: Emissions, transport, transformation, deposition and assessment, *EM*, 22– 25.
- Aneja, V.P., P.A. Roelle, G.C. Murray, J. Southerland, J.W. Erisman, D. Fowler, W.A.H. Asman, and N. Patni. (2001). Atmospheric nitrogen compounds II: emissions, transport, transformation, deposition, and assessment. *Atmospheric Environment*, 35: 1903-1911.
- Arya, S. P. S. (1999), *Air pollution meteorology and dispersion*, Oxford University Press, New York.
- Appel, Wyat & Gilliam, R.C. & Pleim, Jonathan & Pouliot, George & Wong, D & Hogrefe, C & Roselle, S.J. & Mathur, R. (2014). Improvements to the WRF-CMAQ modeling system for fine-scale air quality simulations. *EM: Air and Waste Management Association's Magazine for Environmental Managers*. 16-21.
- Asman, W. A. H., M. A. Sutton, and J. K. Schjorring (1998), Ammonia/nitrogen: emission, atmospheric transport and deposition, *New Phytologist*, 139(1), 27–48, doi:10.1046/j.1469-8137.1998.00180.x.
- Baek, B. H., Todd, R., Cole, N. A., & Koziel, J. A. (2006). Ammonia/nitrogen and hydrogen sulfide flux and dry deposition velocity estimates using vertical gradient method at a commercial beef cattle feedlot. *International Journal of Global Environmental Issues*, 6, 189-203.
- Baek, B.H. and V.P. Aneja (2004), Measurement and analysis of the relationship between ammonia/nitrogen, acid gas, and fine particulates in eastern North Carolina, *Journal of Air & Waste Management. Association*, 54(5), 623-633.
- Bajwa, K. S., and V. P. Aneja (2008), Modeling studies of ammonia/nitrogen dispersion and dry deposition at some hog farms in North Carolina, *Journal of Air & Waste Management Association*, 58, 1198–1207, doi:10.3155/1047-3289.58.9.1198.
- Battye, W., V. P. Aneja, and W. H. Schlesinger (2017), Is nitrogen the next carbon?, *Earth's Future*, 5(9), 894–904, doi:10.1002/2017ef000592.
- Benedict, K. B., C. M. Carrico, S.M. Kreidenweis, B. Schichtel, W. C. Malm, & J. L. Collett, Jr. (2013). A seasonal nitrogen deposition budget for Rocky Mountain National Park. *Ecological Applications*, 23(5), 1156-1169.
- Bittman, S., and R. Mikkelsen (2009), Ammonia/nitrogen emissions from agricultural operations: livestock, *Poultry Sciences*, 54(6), 28–32.

- Briggs, G. A. (1993), Plume Dispersion in the Convective Boundary Layer. Part II: Analyses of CONDORS Field Experiment Data, *Journal of Applied Meteorology*, 32(8), 1388–1425, doi:10.1175/1520-0450(1993)032<1388:pditcb>2.0.co;2.
- Buitjes, P., F. S. Banzha., T. Gauger, E. Hend riks, A. Kerschbaumer, M. Koenen, H. D. Nagel, M. Schaap, et al. (2011). Erfassung, Prognose und Bewertung von Stoffeinträgen und ihren Wirkungen in Deutschland (in German language). *Report of the German Federal Environmental Agency (UBA)*, FKZ 3707 64 200.
- Burns, R. T., H. Xin, R. Gates, H. Li, D. Overhults, L. B. Moody, and J. Ernest (2007), Ammonia/nitrogen Emissions from Poultry Houses in the Southeastern United States, *International Symposium on Air Quality and Waste Management for Agriculture, 16-19 September 2007*, Broomfield, Colorado, doi:10.13031/2013.23882.
- Chamberlain (1953), A General Gaussian Diffusion-Deposition Model for Elevated Point Sources, *Journal of Applied Meteorology*, 15(11), 1167–1171, doi:10.1175/1520-0450(1976)015<1167:aggddm>2.0.co;2.
- Cimorelli, A.J.; S. G. Perry; A. Venktaram, J. C. Weil; R. J. Paine; R. B. Wilson; R. F. Lee; W. D. Peters; R. W. (2005), AERMOD. A Dispersion Model for Industrial Source Applications Part 1: General Model Formulation and Boundary Layer Characterization. *Journal of Applied Meteorology*, 44, 682-693.
- Cooter, E. J., J. O. Bash, J. T. Walker, M. Jones, and W. Robarge (2010), Estimation of NH₃ bi-directional flux from managed agricultural soils, *Atmospheric Environment*, 44(17), 2107–2115, doi:10.1016/j.atmosenv.2010.02.044.
- Deardorff, J. W., and G. E. Willis (1985), Further results from a laboratory model of the convective planetary boundary layer, *Boundary-Layer Meteorology*, 32(3), 205–236, doi:10.1007/bf00121880.
- Dennis, R. L., R. Mathur, J. E. Pleim, and J. T. Walker (2010), Fate of ammonia emissions at the local to regional scale as simulated by the Community Multiscale Air Quality model, *Atmospheric Pollution Research*, 1(4), 207–214, doi:10.5094/apr.2010.027.
- Duyzer, J. (1994), Dry deposition of ammonia/nitrogen and ammonium aerosols over heathland, *Journal of Geophysical Research*, 99(D9), 18757, doi:10.1029/94jd01210.
- Farquhar, G. D., P. M. Firth, R. Wetselaar, and B. Weir (1980), On the Gaseous Exchange of Ammonia between Leaves and the Environment: Determination of the Ammonia Compensation Point, *Plant Physiology*, 66(4), 710–714, doi:10.1104/pp.66.4.710.
- Gates, R. S., H. Xin, K. D. Casey, Y. Liang, and E. F. Wheeler (2005), Method for Measuring Ammonia/nitrogen Emissions from Poultry Houses, *The Journal of Applied Poultry Research*, 14(3), 622–634, doi:10.1093/japr/14.3.622.

- Gilbert, P. M., R. Magnien, M. W. Lomas, J. Alexander, C. Fan, E. Haramoto, T. M. Trice, T. M. Kana (2001). Harmful algal blooms in the Chesapeake and Coastal Bays of Maryland, USA: Comparisons of 1997, 1998, and 1999 events. *Estuaries*. 2001(24), 875–883.
- Hall, D. J., Spanton, A.M., Dunkerley, F., Bennett, M., Griffiths, R.F., (2000). *An InterComparison of the AERMOD, ADMS and ISC Dispersion Models for Regulatory Applications*. Report No. P362. Environment Agency, Bristol, UK.
- Hanna, S.R., B.A. Egan, J. Purdum, J. Wagler., (2001). Evaluation of the ADMS, AERMOD, and ISC3 dispersion models with the OPTEX, Duke Forest, Kincaid, Indianapolis and Lovett field datasets. *International Journal of Environmental Pollution*. 16 (1), 301-314.
- Hayashi, K., K. Ono, T. Tokida, T. Takimoto, M. Mano, A. Miyata, and K. Matsuda (2012), Atmosphere-rice paddy exchanges of inorganic particles and relevant gases during a week in winter and a week in summer, *Journal of Agricultural Meteorology*, 68(1), 55–68, doi:10.2480/agrmet.68.1.8.
- Irwin, J. S. (2013), A suggested method for dispersion model evaluation, *Journal of the Air & Waste Management Association*, 64(3), 255–264, doi:10.1080/10962247.2013.833147.
- Jacobson, M. Z. (1999), *Fundamentals of atmospheric modeling*, Cambridge University Press, Cambridge, UK.
- James, K. M., J. Blunden, I. C. Rumsey, and V. P. Aneja (2012), Characterizing ammonia/nitrogen emissions from a commercial mechanically ventilated swine finishing facility and an anaerobic waste lagoon in North Carolina, *Atmospheric Pollution Research*, 3(3), 279–288, doi:10.5094/apr.2012.031.
- Jitra, N., N. Pinthong, and S. Thepanondh (2015), Performance Evaluation of AERMOD and CALPUFF Air Dispersion Models in Industrial Complex Area, *Air, Soil and Water Research*, 8, doi:10.4137/aswr.s32781.
- Jones, M.R., Leith, I.D., Fowler, D., Raven, J.A., Sutton, M.A., Nemitz, E., Cape, J.N., Sheppard, L.J., Smith, R.I., Theobald, M.R., 2007. Concentration-dependent NH₃ deposition processes for mixed moorland semi-natural vegetation. *Atmospheric Environment* 41, 2049-2060
- Katata, G., K. Hayashi, K. Ono, H. Nagai, A. Miyata, and M. Mano (2013), Coupling atmospheric ammonia/nitrogen exchange process over a rice paddy field with a multi-layer atmosphere-soil-vegetation model, *Agricultural and Forest Meteorology*, 180, 1–21, doi:10.1016/j.agrformet.2013.05.001.
- Khoirunissa, I. (2018), Performance of AERMOD Modelling of Hydrogen Sulfide (H₂S) Concentration from Geothermal Power Plants in Ulubelu, Indonesia and Hellisheidi-Nesjavellir, Iceland, *UNU-GTP 40th Anniversary Workshop*.

- Kirchner, M., G. Jakobi, E. Feicht, M. Bernhardt, and A. Fischer (2005), Elevated NH₃ and NO₂ air concentrations and nitrogen deposition rates in the vicinity of a highway in Southern Bavaria, *Atmospheric Environment*, 39(25), 4531–4542, doi:10.1016/j.atmosenv.2005.03.052.
- Krupa, S.V. (2003). Effects of atmospheric ammonia/nitrogen (NH₃) on terrestrial vegetation: Review. *Environmental Pollution* 124: 179-221.
- Larsen, R. K., J. C. Steinbacher, and J. E. Baker (2001), Ammonia/nitrogen Exchange between the Atmosphere and the Surface Waters at Two Locations in the Chesapeake Bay, *Environmental Science & Technology*, 35(24), 4731–4738, doi:10.1021/es0107551.
- Linker, Lewis C., Robin Dennis, Gary W. Shenk, Richard A. Batiuk, Jeffrey Grimm, and Ping Wang, (2013). Computing Atmospheric Nutrient Loads to the Chesapeake Bay Watershed and Tidal Waters. *Journal of the American Water Resources Association (JAWRA)* 1-17. DOI: 10.1111/jawr.12112
- Meyers, T., W. Luke, and J. Meisinger (2006), Fluxes of ammonia/nitrogen and sulfate over maize using relaxed eddy accumulation, *Agricultural and Forest Meteorology*, 136(3-4), 203–213, doi:10.1016/j.agrformet.2004.10.005.
- Myles, L., J. Kochendorfer, M. W. Heuer, and T. P. Meyers (2011), Measurement of Trace Gas Fluxes over an Unfertilized Agricultural Field Using the Flux-gradient Technique, *Journal of Environment Quality*, 40(5), 1359, doi:10.2134/jeq2009.0386.
- National Research Council. (2003). *Air Emissions from Animal Feeding Operations: Current Knowledge, Future Needs*. National Academy Press, Washington, DC. ISBN: 0-309-08705-8
- Neirynck, J., A. Kowalski, A. Carrara, and R. Ceulemans (2005), Driving forces for ammonia/nitrogen fluxes over mixed forest subjected to high deposition loads, *Atmospheric Environment*, 39(28), 5013–5024, doi:10.1016/j.atmosenv.2005.05.027.
- Neirynck, J., A. Kowalski, A. Carrara, G. Genouw, P. Berghmans, and R. Ceulemans (2007), Fluxes of oxidised and reduced nitrogen above a mixed coniferous forest exposed to various nitrogen emission sources, *Environmental Pollution*, 149(1), 31–43, doi:10.1016/j.envpol.2006.12.029.
- Nus, J., and M. Kenna (2012), *Nutrient Fate and Transport*, Green Section Record, 50(5).
- O'Shaughnessy, P. T., and R. Altmaier (2011), Use of AERMOD to determine a hydrogen sulfide emission factor for swine operations by inverse modeling, *Atmospheric Environment*, 45(27), 4617–4625, doi:10.1016/j.atmosenv.2011.05.061.

- Peters, W. D. (2015), *AERMOD: description of model formulation*, U.S. Environmental Protection Agency, Office of Air Quality Planning and Standards, Emissions Monitoring and Analysis Division, Research Triangle Park, NC.
- Phillips, S. (2004), Ammonia/nitrogen flux and dry deposition velocity from near-surface concentration gradient measurements over a grass surface in North Carolina, *Atmospheric Environment*, 38(21), 3469–3480, doi:10.1016/s1352-2310(04)00245-6.
- Pleim, J. E., J. O. Bash, J. T. Walker, and E. J. Cooter (2013), Development and evaluation of an ammonia/nitrogen bidirectional flux parameterization for air quality models, *Journal of Geophysical Research: Atmospheres*, 118(9), 3794–3806, doi:10.1002/jgrd.50262.
- Redwine, J. S., and R. E. Lacey (2001), *Concentration and Emissions of Ammonia and Particulate Matter in Tunnel Ventilated Broiler Houses under Summer Conditions in Texas, 2001 Sacramento, CA July 29-August 1, 2001*, doi:10.13031/2013.3540.
- Sander, R. (2015), Compilation of Henrys law constants (version 4.0) for water as solvent, *Atmospheric Chemistry and Physics*, 15(8), 4399–4981, doi:10.5194/acp-15-4399-2015.
- Schlossberg, T. (2017). *Fertilizers, a Boon to Agriculture, Pose Growing Threat to U.S. Waterways*, New York Times, July 27, 2017.
- Schrader, F., and C. Brümmer (2014), Land Use Specific Ammonia Deposition Velocities: a Review of Recent Studies (2004–2013), *Water, Air, & Soil Pollution*, 225(10), doi:10.1007/s11270-014-2114-7.
- Seinfeld, John H.; Pandis, Spyros N (2016), *Atmospheric Chemistry and Physics*, Wiley.
- Sheeder, S. A., J. A. Lynch, and J. Grimm (2002), Modeling Atmospheric Nitrogen Deposition and Transport in the Chesapeake Bay Watershed, *Journal of Environment Quality*, 31(4), 1194, doi:10.2134/jeq2002.1194.
- Shen, J., D. Chen, M. Bai, J. Sun, T. Coates, S. K. Lam, and Y. Li (2016), Ammonia/nitrogen deposition in the neighbourhood of an intensive cattle feedlot in Victoria, Australia, *Scientific Reports*, 6(1), doi:10.1038/srep32793.
- Siefert, R. L., J. R. Scudlark, A. G. Potter, K. A. Simonsen, and K. B. Savidge. (2004). Characterization of Atmospheric Ammonia Emissions from a commercial chicken house on the Delmarva Peninsula. *Environmental Science & Technology*, 38(10). 2769-2778.
- Sutton, M. et al. (1998), Dispersion, deposition and impacts of atmospheric ammonia/nitrogen: quantifying local budgets and spatial variability, *Nitrogen*, the Confer-N-s, 349–361, doi:10.1016/b978-0-08-043201-4.50052-6.
- Taylor, G. I. (1922), *Diffusion by Continuous Movements*, Proceedings of the London Mathematical Society, s2-20(1), 196–212, doi:10.1112/plms/s2-20.1.196.

- Theobald, M. R., P. Løfstrøm, J. Walker, H. V. Andersen, P. Pedersen, A. Vallejo, and M. A. Sutton (2012), An intercomparison of models used to simulate the short-range atmospheric dispersion of agricultural ammonia/nitrogen emissions, *Environmental Modelling & Software*, 37, 90–102, doi:10.1016/j.envsoft.2012.03.005.
- Tomich, T.P., S.B. Brodt, R.A. Dahlgren, and K.M. Scow. (2016). *The California Nitrogen Assessment: Challenges and solutions for people, agriculture, and the environment*, The University of California Press, p. 304.
- U.S. Environmental Protection Agency (2010), *2011 National Emission Inventory (NEI) Report*, 1-23. Retrieved from <https://www.epa.gov/air-emissions-inventories/2011-national-emissions-inventory-nei-data>.
- U.S. Environmental Protection Agency (2013), *AERMOD and AERMET, Air Dispersion Modeling*, 491–513, doi:10.1002/9781118723098.ch14.
- U.S. Environmental Protection Agency. (2014). *Chesapeake Bay Total Maximum Daily Load (TMDL)*. Retrieved from <https://www.epa.gov/chesapeake-bay-tmdl>.
- Walker, J. T., V. P. Aneja, and D. A. Dickey (2000), Atmospheric transport and wet deposition of ammonium in North Carolina, *Atmospheric Environment*, 34(20), 3407–3418, doi:10.1016/s1352-2310(99)00499-9.
- Walker, J., P. Spence, S. Kimbrough, and W. Robarge (2008), Inferential model estimates of ammonia dry deposition in the vicinity of a swine production facility, *Atmospheric Environment*, 42(14), 3407–3418, doi:10.1016/j.atmosenv.2007.06.004.
- Wesely, M. L., P. V. Doskey, and J. D. Shannon (2002), *Deposition parameterizations for the Industrial Source Complex (ISC3) model*, , doi:10.2172/1260839.
- Yu, S., B. Eder, R. Dennis, S.-H. Chu, and S. E. Schwartz (2006), New unbiased symmetric metrics for evaluation of air quality models, *Atmospheric Science Letters*, 7(1), 26–34, doi:10.1002/asl.125.
- Zhang, Y., P. Liu, B. Pun, and C. Seigneur (2006), A comprehensive performance evaluation of MM5-CMAQ for the Summer 1999 Southern Oxidants Study episode—Part I: Evaluation protocols, databases, and meteorological predictions, *Atmospheric Environment*, 40(26), 4825–4838, doi:10.1016/j.atmosenv.2005.12.043.

Table 1. Estimated Emissions using CMU Emission Factors, USDA Activity Data for CAFO/Commercial animal populations on the Delmarva Peninsula. Data is used to calculate estimated emissions to show contribution of each animal to the overall ammonia/nitrogen emissions in the Delmarva region. County-level data is used for CMU and USDA data and only the counties in the Delmarva region are used (results for the counties with yellow background in Figure 1).

| Animal | Emission Factor (kg NH ₃ an ⁻¹ year ⁻¹) (CMU, 2004) | Activity/Population* (2012) | Estimated Emissions (kg NH ₃ year ⁻¹) |
|---------|---|--------------------------------|--|
| Poultry | 0.200 | 553,869,560 | 110,773,912 |
| Layers | 0.558 | 10,692 | 5,966 |
| Dairy | 19.176 | 12,661 | 242,787 |
| Beef | 19.960 | 7,296 | 145,628 |
| Swine | 9.982 | 428 | 4,272 |

* Activity/Population is standing animal population at any given time. Inventory refers to the total animal population per year.

Table 2. CMU Emission Factors subdivided into activity type. Each activity type's total emission factor has three contributing sources of emission including confinement, storage, and land application. In many cases, the emission factor will vary based on waste management practice. The most common management practice has been assumed in this case based on activity availability from CMU.

| Activity Type | Confinement (kg NH ₃ an ⁻¹ mo ⁻¹) | Storage (kg NH ₃ an ⁻¹ mo ⁻¹) | Land Application (kg NH ₃ an ⁻¹ mo ⁻¹) | Total (kg NH ₃ an ⁻¹ yr ⁻¹) |
|---------------|---|---|--|---|
| Poultry | 0.00832 | 0.001510 | 0.00680 | 0.200 |
| Layer | 0.00945 | 0.031800 | 0.00529 | 0.558 |
| Dairy | 0.68000 | 0.011000 | 0.90700 | 19.176 |
| Beef | 0.94500 | 0.000378 | 0.71800 | 19.960 |
| Swine | 0.22700 | 0.567000 | 0.03780 | 9.982 |

Table 3. A summary of measured deposition velocities for selected studies (located in the reference column). Deposition velocities based on studies in previous years. Site indicates the area in which the measurements were taken. Deposition velocities are measured at these sites and may vary based on method of measurement and regional sources of ammonia/nitrogen. Season/time indicate the season and time of day for which the experiment was intended. Many values included by Schrader and Brummer (2014).

| Reference | Site | Deposition Velocity (cm/s) | Season / Time |
|-------------------------------|----------------------------|-------------------------------|-----------------------------|
| Bajwa et al. (2008) | Semi-Natural | 0.8 | Fall, Daytime |
| | | 0.6 | Annual Mean |
| Phillips et al. (2004) | Semi-Natural (<i>ag</i>) | 2.8 | Fall, Daytime |
| | | 1.7 | Annual Mean |
| Myles et al. (2011) | Semi-Natural | 1.8 | Annual Mean |
| Benedict et al. (2013) | Semi-Natural | 1.2 (0.1 – 2.3) | Annual Mean (Range) |
| Kirchner et al. (2005) | Semi-Natural | 1.4 (0.5 – 2.2) | Annual Mean (Range) |
| Neirynck et al. (2005) | Mixed Forests | 3.5 | Summertime, Daytime |
| | | 2.4 | Summertime, Nighttime |
| Neirynck et al. (2007) | Mixed Forests | 2.8 | Summer, Daytime |
| | | 3.0 | Annual Mean |
| Baek et al. (2006) | Agriculture | 6.3 | Summer, Daytime |
| Builtjes et al. (2011) | Agriculture | 1.6 | Mean at Reference Height |
| | | 0.6 | Winter, Daytime |
| Hayashi et al. (2012) | Agriculture | 0.2 | Summer Crop, Daytime |
| | | 0.3 | Annual Mean |
| Katata et al. (2013) | Agriculture | 0.2 – 1.0 | Crop Growth Period Averages |
| | | 0.6 | Annual Mean |
| Meyers et al. (2006) | Agriculture | 4.7 | Summer, Daytime |
| Myles et al. (2011) | Agriculture | 7.1 | Fall, Daytime |
| | | 2.2 | Annual Mean |

Table 4. A summary of site characteristics describing nearby structures, trees, and potential ammonia/nitrogen sources. In the left column is the site number (note: #17 unused). The description simply defines the site as either Residential, Rural, Commercial, or Marine. This gives more detail as to what potential sources could exist.

| # | Description | Site Features |
|----|--------------|---|
| 1 | Residential | Trees surrounding sampler, 30 feet from structure, creek/inlet next to the sampler. |
| 2 | Residential | Open area approximately 20 feet from structure, no shade, standing water present. |
| 3 | Rural | Next to Bay, standing water present, compost storage nearby. |
| 4 | Residential | Approximately 40 feet from river, constant thermally forced breeze, removed from structures/trees. |
| 5 | Residential | Under canopy of trees surrounding site, garden next to site, no sun. |
| 6 | Marine | Next to Bay, constant thermally forced breeze, removed from structures/trees. |
| 7 | Residential | Surrounded by trees, next to the river, fire pit next to the sampler, no sun. |
| 8 | Agricultural | Next to a soybean field, about 15 feet from a structure, open area, mostly shaded. |
| 9 | Agricultural | Middle of a field, no obstructions, no obvious sources of ammonia/nitrogen. |
| 10 | Commercial | On patio where employees visit, non-natural ground, next to a small tree, no notable sources. |
| 11 | Residential | Sampler placed in an inactive garden, next to a fence, underneath a tree, no fertilizer used in garden. |
| 12 | Residential | Next to the road, next to a flower garden, water did contaminate sensor. |
| 13 | Residential | Open and away from structures, small trees nearby, lawn manicured. |
| 14 | Residential | Next to the water, tall grass around with no trees and no structures. |
| 15 | Agricultural | No obvious obstructions, no shade. |
| 16 | Residential | Sampler placed in large clearing near wolf statues, no obvious structures, lawn manicured. |
| 18 | Residential | Shed nearby, no trees near sampler, approximately 40 feet from house. |
| 21 | | Tall grass, swampy, standing estuary water observed each time we visited, vehicle traffic is likely nearby. |
| 22 | Residential | Away from trees, away from structures, near gravel road, we were notified that pet waste was a possibility. |
| 23 | Agricultural | Corner of a large grass field, next to a garden, possible farm traffic, no structures. |

Table 5. A summary of sampled ammonia mass and concentrations for Trip 1 (September 8, 2017 – September 22, 2017). The column on the left indicates the sampler number (#). Column two indicates Sampler ID which is defined as either a laboratory blank (LB), travel blank (TB), or a sampler deployed in the field (number). The mass is extracted and reported and then applied a conversion based on the effective volume of the sampler and the time of exposure in seconds. Concentration in parts per billion (ppb) is included in the last column with concentrations of samplers deployed in the field being the difference of the converted concentrations minus the average of the travel blank concentrations (0.162 ppb).

| # | Sampler ID | Sampler Date | NH ₃ Mass (μg) | NH ₃ Concentration ($\mu\text{g m}^{-3}$) | NH ₃ Concentration (ppb) |
|--------------------|------------|-------------------|---|---|--|
| 1 | LB | 12-Sep-17 | 0.045 | 0.031 | 0.042 |
| 2 | LB | 12-Sep-17 | 0.056 | 0.039 | 0.053 |
| 3 | LB | 12-Sep-17 | 0.043 | 0.029 | 0.040 |
| 4 | LB | 12-Sep-17 | 0.056 | 0.039 | 0.053 |
| 5 | LB | 12-Sep-17 | 0.056 | 0.039 | 0.053 |
| 6 | LB | 12-Sep-17 | 0.053 | 0.036 | 0.049 |
| 7 | LB | 12-Sep-17 | 0.043 | 0.029 | 0.040 |
| 8 | LB | 12-Sep-17 | 0.031 | 0.021 | 0.029 |
| 22 | 1 | 26-Sep-17 | 0.875 | 0.600 | 0.656 |
| 23 | 2 | 26-Sep-17 | 1.692 | 1.159 | 1.419 |
| 24 | 3 | 26-Sep-17 | 1.633 | 1.119 | 1.365 |
| 25 | 4 | 26-Sep-17 | 1.050 | 0.719 | 0.820 |
| 26 | 5 | 26-Sep-17 | 1.944 | 1.332 | 1.656 |
| 27 | 6 | 26-Sep-17 | 1.206 | 0.826 | 0.965 |
| 28 | 7 | 26-Sep-17 | 4.861 | 3.331 | 4.382 |
| 29 | 8 | 26-Sep-17 | 1.711 | 1.173 | 1.438 |
| 30 | 9 | 26-Sep-17 | 1.517 | 1.039 | 1.256 |
| 31 | 10 | 26-Sep-17 | 1.925 | 1.319 | 1.638 |
| 32 | 11 | 26-Sep-17 | 2.139 | 1.466 | 1.838 |
| 33 | 12 | 26-Sep-17 | 5.250 | 3.597 | 4.746 |
| 34 | 13 | 26-Sep-17 | 1.342 | 0.919 | 1.092 |
| 35 | 14 | 26-Sep-17 | 1.031 | 0.706 | 0.801 |
| 40 | 15 | 26-Sep-17 | 3.306 | 2.265 | 2.928 |
| 41 | 16 | 26-Sep-17 | 0.914 | 0.626 | 0.692 |
| 42 | 17 | 26-Sep-17 | 1.167 | 0.799 | 0.929 |
| 43 | 18 | 26-Sep-17 | 1.050 | 0.719 | 0.820 |
| 44 | 19 | 26-Sep-17 | 0.914 | 0.626 | 0.692 |
| 45 | 20 | 26-Sep-17 | 4.861 | 3.331 | 4.382 |
| 46 | 21 | 26-Sep-17 | 1.283 | 0.879 | 1.038 |
| 47 | 22 | 26-Sep-17 | 0.992 | 0.680 | 0.765 |
| 48 | 23 | 26-Sep-17 | 1.536 | 1.053 | 1.274 |
| 36 | TB1 | 26-Sep-17 | 0.194 | 0.133 | 0.182 |
| 37 | TB2 | 26-Sep-17 | 0.169 | 0.116 | 0.158 |
| 38 | TB3 | 26-Sep-17 | 0.140 | 0.096 | 0.131 |
| 39 | TB4 | 26-Sep-17 | 0.138 | 0.095 | 0.129 |
| 54 | TB5 | 26-Sep-17 | 0.171 | 0.117 | 0.160 |
| 55 | TB6 | 26-Sep-17 | 0.253 | 0.173 | 0.236 |
| 56 | TB7 | 26-Sep-17 | 0.159 | 0.109 | 0.149 |
| 57 | TB8 | 26-Sep-17 | 0.214 | 0.147 | 0.200 |
| 62 | TB9 | 26-Sep-17 | 0.152 | 0.104 | 0.142 |
| 63 | TB10 | 26-Sep-17 | 0.144 | 0.099 | 0.135 |
| Stats (ppb) | | Lab Blanks | | Travel Blanks | Deployed Samplers |
| Mean | | 0.045 | | 0.162 | 1.796 |
| STD | | 0.008 | | 0.033 | 1.216 |
| Median | | 0.046 | | 0.154 | 1.418 |
| Max | | 0.053 | | 0.236 | 4.908 |
| Min | | 0.029 | | 0.129 | 0.818 |

Table 6. A summary of sampled ammonia mass and concentrations for Trip 2 (September 22, 2017 – October 6, 2017). The column on the left indicates the sampler number (#). Column two indicates Sampler ID which is defined as either a laboratory blank (LB), travel blank (TB), or a sampler deployed in the field (number). The mass is extracted and reported and then applied a conversion based on the effective volume of the sampler and the time of exposure in seconds. Concentration in parts per billion (ppb) is included in the last column with concentrations of samplers deployed in the field being the difference of the converted concentrations minus the average of the travel blank concentrations (0.114 ppb).

| # | Sampler ID | Sampler Date | NH ₃ Mass (μg) | NH ₃ Concentration ($\mu\text{g m}^{-3}$) | NH ₃ Concentration (ppb) |
|--------------------|------------|--------------|---|---|--|
| 95 | LB | 9-Oct-17 | 0.054 | 0.037 | 0.051 |
| 96 | LB | 9-Oct-17 | 0.062 | 0.043 | 0.058 |
| 97 | LB | 9-Oct-17 | 0.068 | 0.047 | 0.064 |
| 98 | LB | 9-Oct-17 | 0.070 | 0.048 | 0.065 |
| 99 | LB | 9-Oct-17 | 0.088 | 0.060 | 0.082 |
| 100 | LB | 9-Oct-17 | 0.097 | 0.067 | 0.091 |
| 64 | 1 | 9-Oct-17 | 0.894 | 0.613 | 0.722 |
| 65 | 2 | 9-Oct-17 | 1.653 | 1.133 | 1.431 |
| 66 | 3 | 9-Oct-17 | 1.381 | 0.946 | 1.177 |
| 67 | 4 | 9-Oct-17 | 1.031 | 0.706 | 0.849 |
| 68 | 5 | 9-Oct-17 | 1.517 | 1.039 | 1.304 |
| 69 | 6 | 9-Oct-17 | 1.517 | 1.039 | 1.304 |
| 70 | 7 | 9-Oct-17 | 1.478 | 1.013 | 1.267 |
| 71 | 8 | 9-Oct-17 | 1.886 | 1.292 | 1.649 |
| 72 | 9 | 9-Oct-17 | 1.867 | 1.279 | 1.631 |
| 73 | 10 | 9-Oct-17 | 1.769 | 1.212 | 1.540 |
| 74 | 11 | 9-Oct-17 | 1.944 | 1.332 | 1.704 |
| 75 | 12 | 9-Oct-17 | 1.944 | 1.332 | 1.704 |
| 76 | 13 | 9-Oct-17 | 1.478 | 1.013 | 1.267 |
| 77 | 14 | 9-Oct-17 | 1.128 | 0.773 | 0.940 |
| 82 | 15 | 9-Oct-17 | 2.139 | 1.466 | 1.886 |
| 83 | 16 | 9-Oct-17 | 1.419 | 0.973 | 1.213 |
| 84 | 17 | 9-Oct-17 | 1.342 | 0.919 | 1.140 |
| 85 | 18 | 9-Oct-17 | 1.381 | 0.946 | 1.177 |
| 86 | 19 | 9-Oct-17 | 1.322 | 0.906 | 1.122 |
| 87 | 20 | 9-Oct-17 | 1.439 | 0.986 | 1.231 |
| 88 | 21 | 9-Oct-17 | 1.944 | 1.332 | 1.704 |
| 89 | 22 | 9-Oct-17 | 2.333 | 1.599 | 2.067 |
| 90 | 23 | 9-Oct-17 | 1.614 | 1.106 | 1.395 |
| 78 | TB1 | 9-Oct-17 | 0.117 | 0.080 | 0.109 |
| 79 | TB2 | 9-Oct-17 | 0.119 | 0.081 | 0.111 |
| 80 | TB3 | 9-Oct-17 | 0.105 | 0.072 | 0.098 |
| 81 | TB4 | 9-Oct-17 | 0.113 | 0.077 | 0.105 |
| 91 | TB5 | 9-Oct-17 | 0.095 | 0.065 | 0.089 |
| 92 | TB6 | 9-Oct-17 | 0.159 | 0.109 | 0.149 |
| 93 | TB7 | 9-Oct-17 | 0.138 | 0.095 | 0.129 |
| 94 | TB8 | 9-Oct-17 | 0.128 | 0.088 | 0.120 |
| Stats (ppb) | | | Lab Blanks | Travel Blanks | Deployed Samplers |
| Mean | | | 0.069 | 0.114 | 1.480 |
| STD | | | 0.014 | 0.018 | 0.323 |
| Median | | | 0.065 | 0.110 | 1.418 |
| Max | | | 0.091 | 0.149 | 2.181 |
| Min | | | 0.051 | 0.089 | 0.836 |

Table 7. Summary of precision of duplicate samplers at site 18. Concentrations are provided for both Trip 1 from September 8, 2017 through September 22, 2017 and Trip 2 from September 22, 2017 through October 6, 2017 in units of parts per billion (ppb). Samplers 18A and 18B represent the samplers placed and site number corresponds to the listed site characteristics in table 4. Percent error is given as a mean of measuring precision of the measurements in the same location.

| Duplicate Samplers at Site 18 | Trip 1 (ppb) | Trip 2 (ppb) |
|-------------------------------|--------------|--------------|
| 18A (18) | 0.982 | 1.291 |
| 18B (19) | 0.854 | 1.236 |
| % Error | 13.9% | 4.4% |

Table 8. Summary of precision of duplicate samplers at site 20. Concentrations are provided for both Trip 1 from September 8, 2017 through September 22, 2017 and Trip 2 from September 22, 2017 through October 6, 2017 in units of parts per billion (ppb). Samplers 20A and 20B represent the samplers placed and site number corresponds to the listed site characteristics in table 4. Percent error is given as a mean of measuring precision of the measurements in the same location. (Q?) represents a possible contamination and a outlier which increases percent error significantly.

| Duplicate Samplers at Site 20 | Trip 1 (ppb) | Trip 2 (ppb) |
|-------------------------------|-------------------|--------------|
| 20A (20) | 4.544 (Q?) | 1.345 |
| 20B (21) | 1.200 | 1.818 |
| % Error | 116.4% | 29.9% |

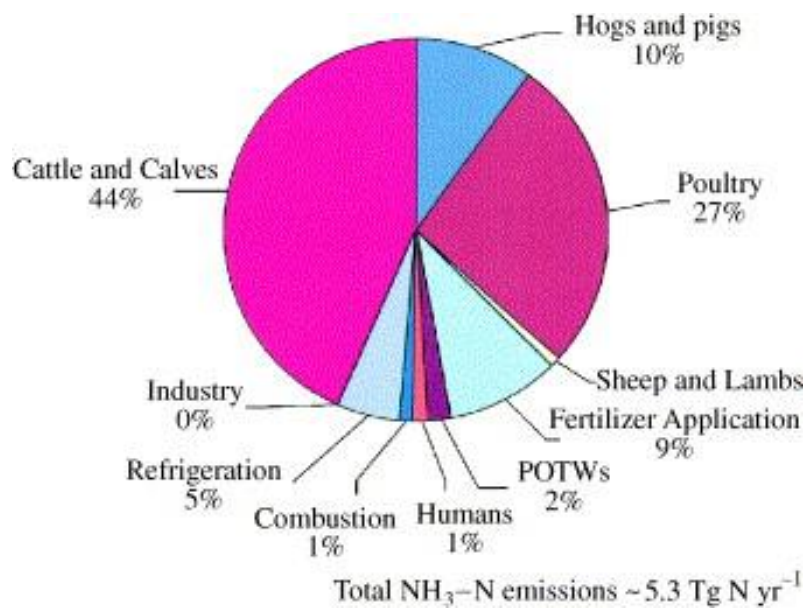


Figure 1. Breakdown of ammonia/nitrogen emissions (in percentage of total $\text{NH}_3\text{-N}$ Tg N yr^{-1}) from various source categories throughout the United States as of 2000 (Source: Aneja et al., 2001).

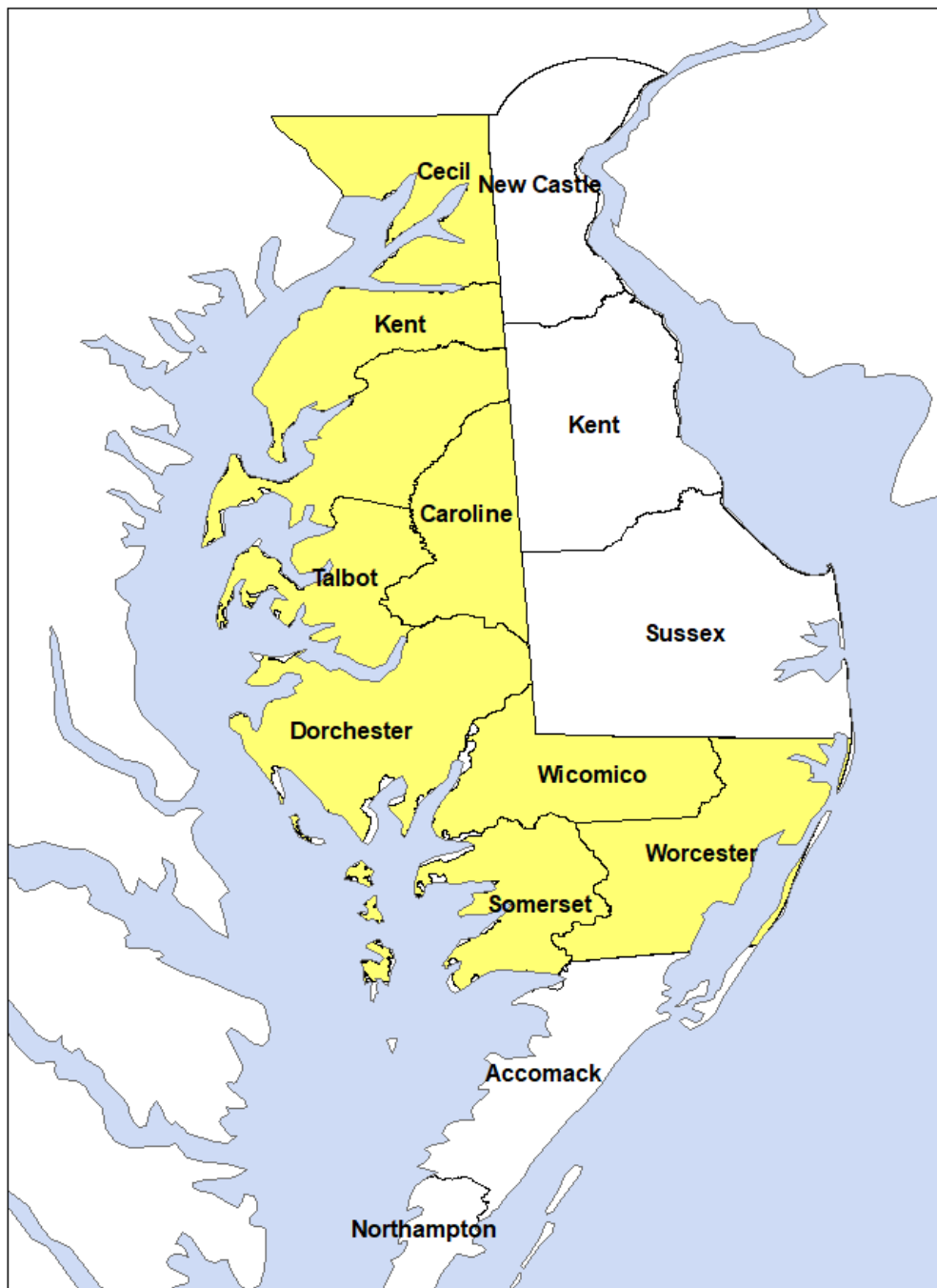


Figure 2. Map of Maryland, Delaware, and Virginia counties on the Chesapeake Bay included in animal population and emission factor calculation. Used as a reference for county-level emissions and calculation throughout the document. (Source: Teach Water Science, 2018). Counties shaded in yellow were the only counties used in the study due to a lack of available data.

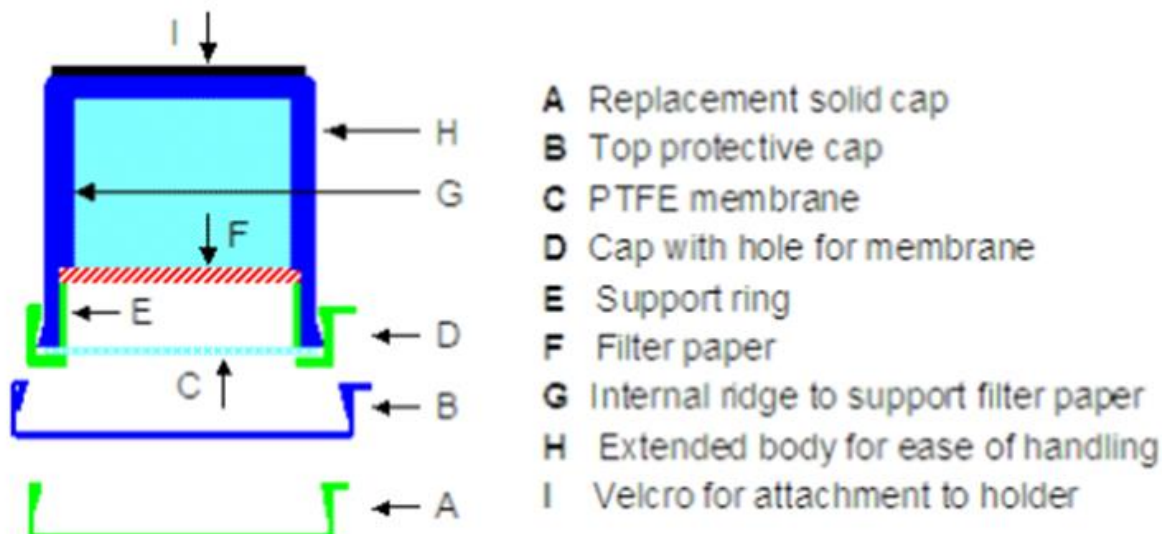


Figure 3: Outline diagram of a single ALPHA Sampler with its components listed.



Figure 4. ALPHA sampler support on a metal post. Pictured on the right is Jordan Baker placing an ALPHA sampler inside the housing. The sampler is inverted with a Velcro strip on the opposite end of the opening. There is another Velcro strip in the housing to which the ALPHA sampler attaches. There is a cage that rotates to catch falling samplers on the underside of the housing. There were no issues with samplers contacting the housing cage during the sampling campaign.

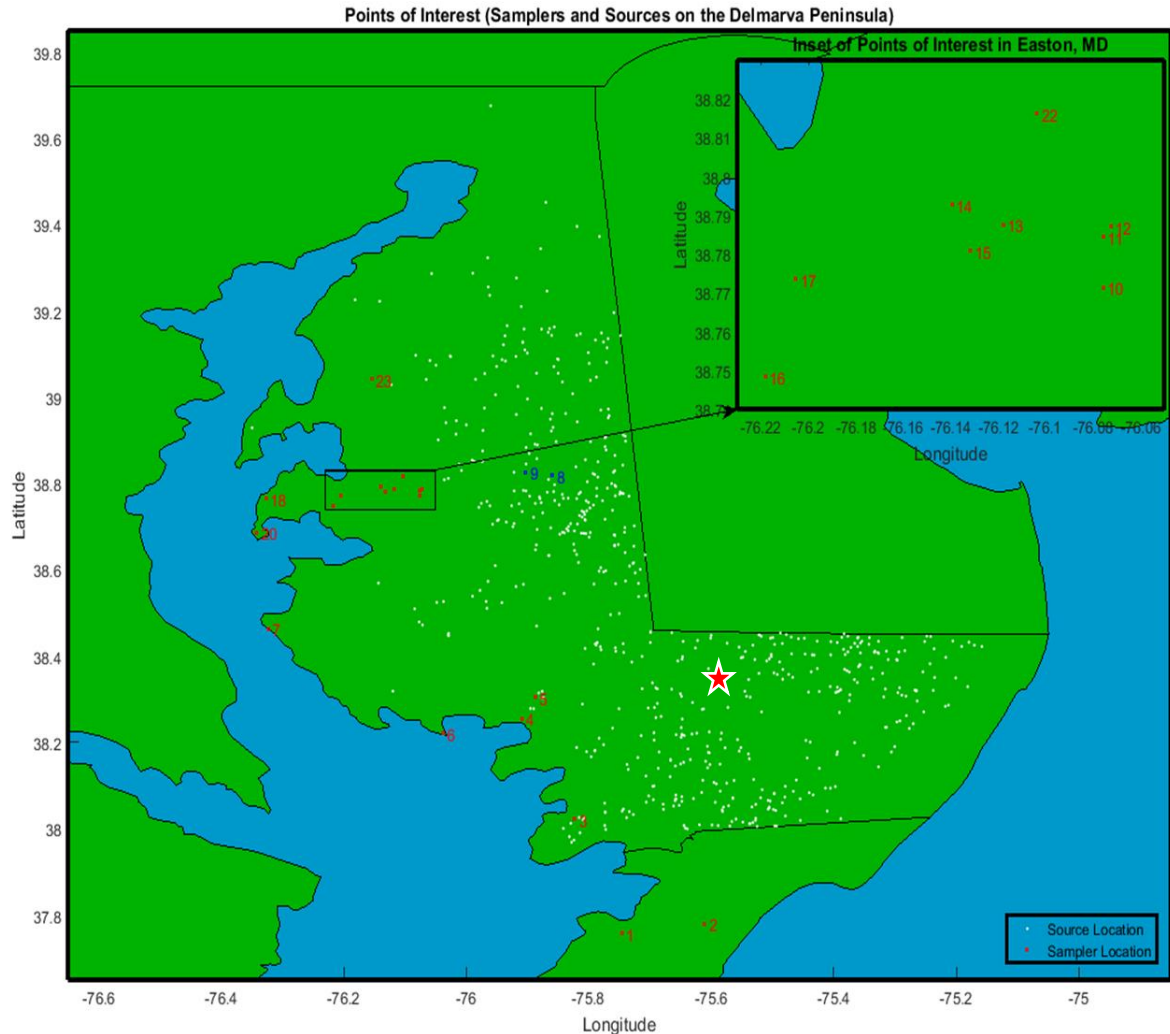


Figure 5. Domain selected in AERMOD for the model simulation. The extent of the model domain is covered by the borders of the edges of the figure. Red locations are areas where samplers were placed. Their number is listed next to the sampler indicator. An inset is provided for an area near Denton and Easton, Maryland where multiple samplers were deployed. White dots indicate areas where current poultry operations reside. There are 720 sources overall with data provided by the MD DOA. The red star indicates the approximate location of KSBY which is also the station from which meteorology data was used.

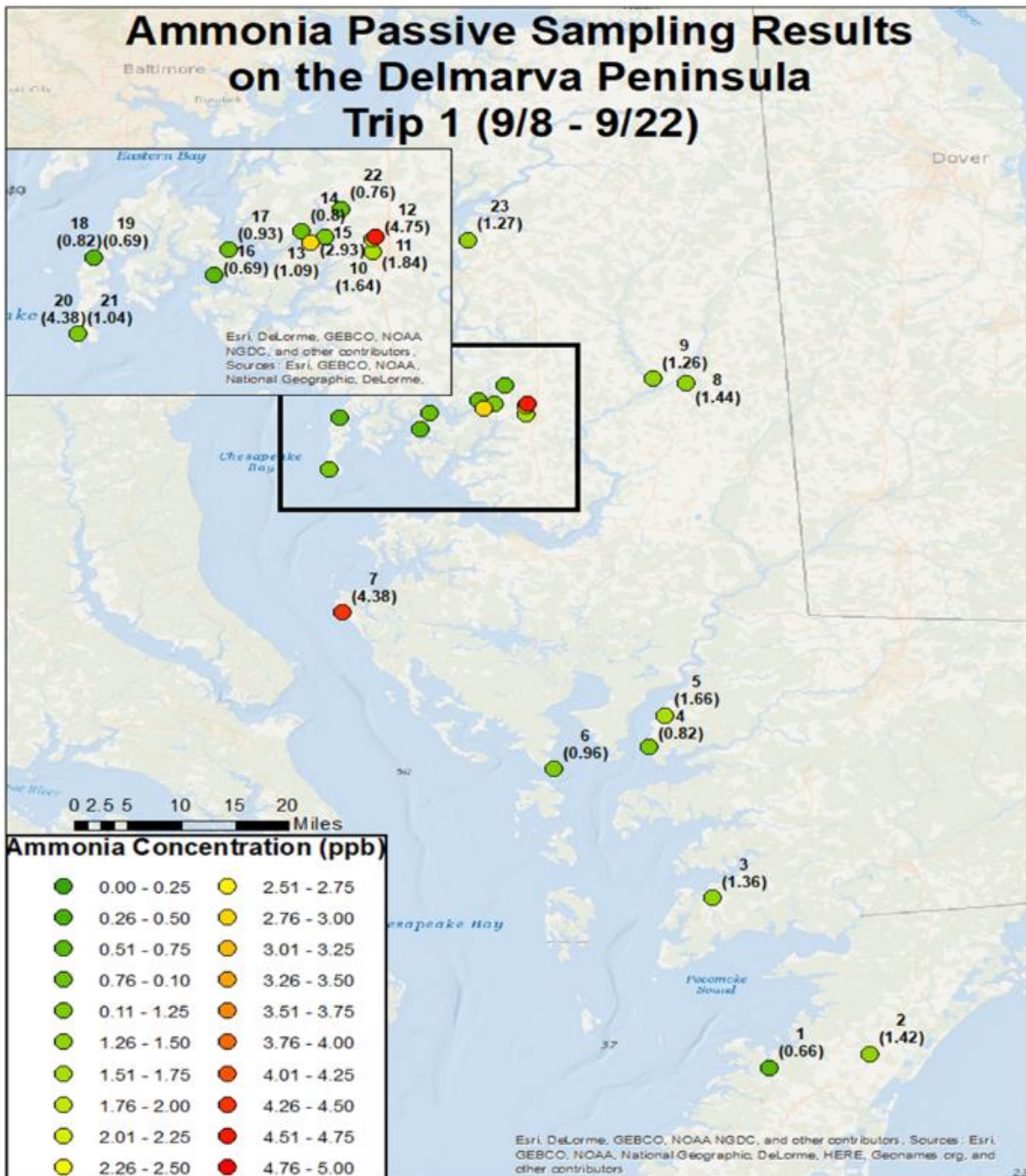


Figure 6. Sampler results shown (for various measurement sites with corresponding concentration) in units of parts per billion of ammonia/nitrogen (ppb). Colors indicate relative strength of the concentration for Trip 1. These are combined in the final concentration calculation in the analysis from AERMOD.

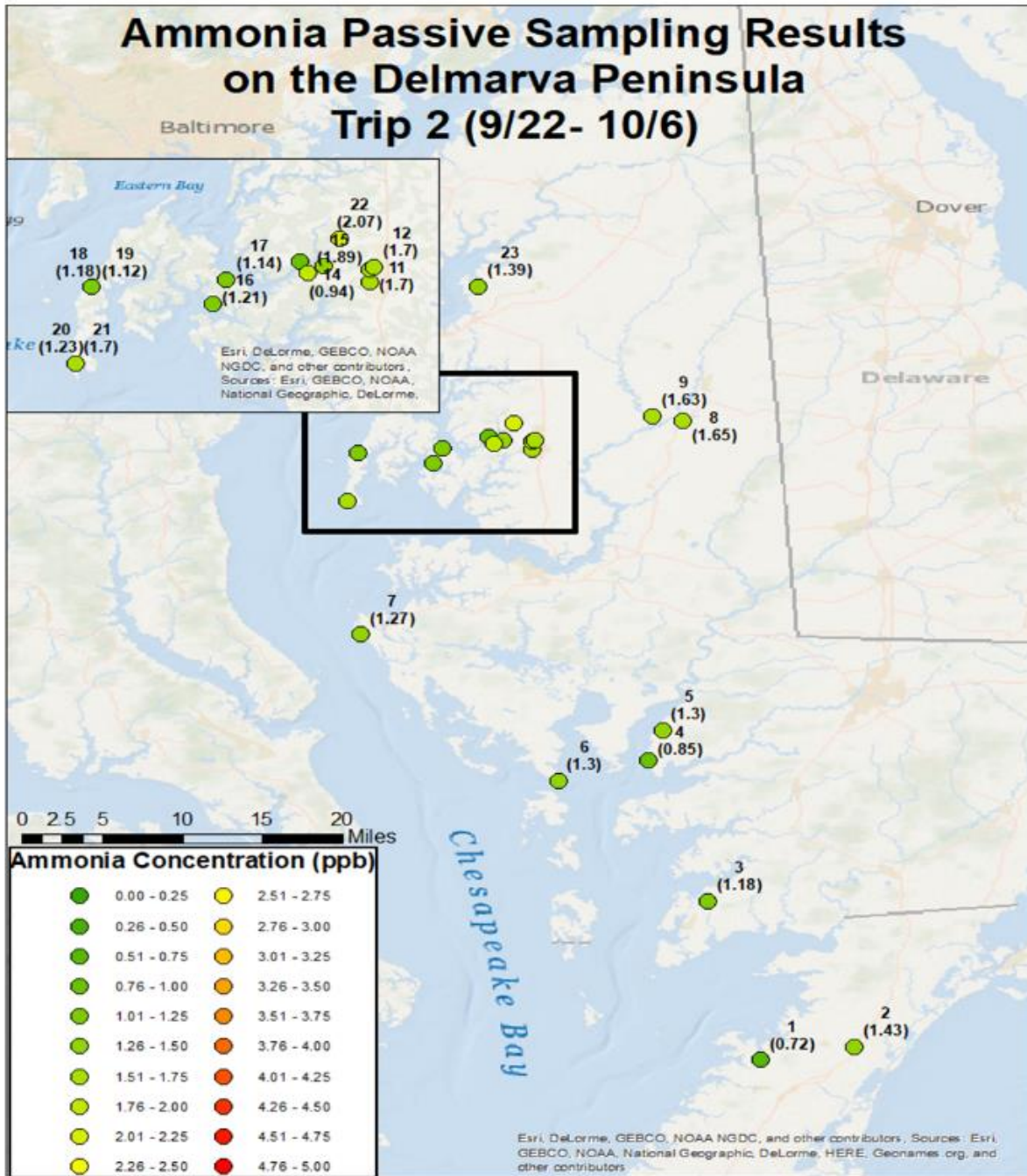


Figure 7. Sampler results shown (for various measurement sites with corresponding concentration) with units of parts per billion of ammonia/nitrogen (ppb). Colors indicate relative strength of the concentration for Trip 2. These are combined in the final concentration calculation in the analysis from AERMOD.

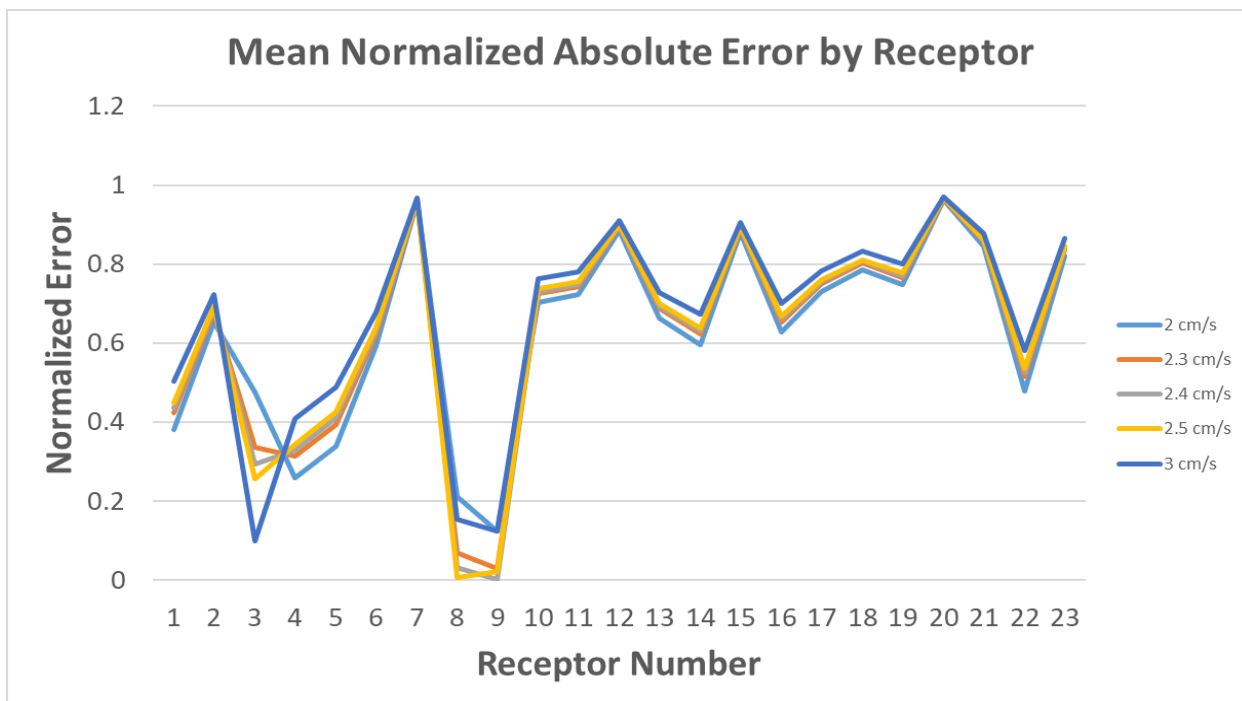


Figure 8. Mean Normalized Absolute Error (MNAE) with values of MNAE on the y-axis as it correlates with receptor on the x-axis. Only deposition velocities of 2, 2.3, 2.4, 2.5, and 3 cm/s are considered in the MNAE calculation.

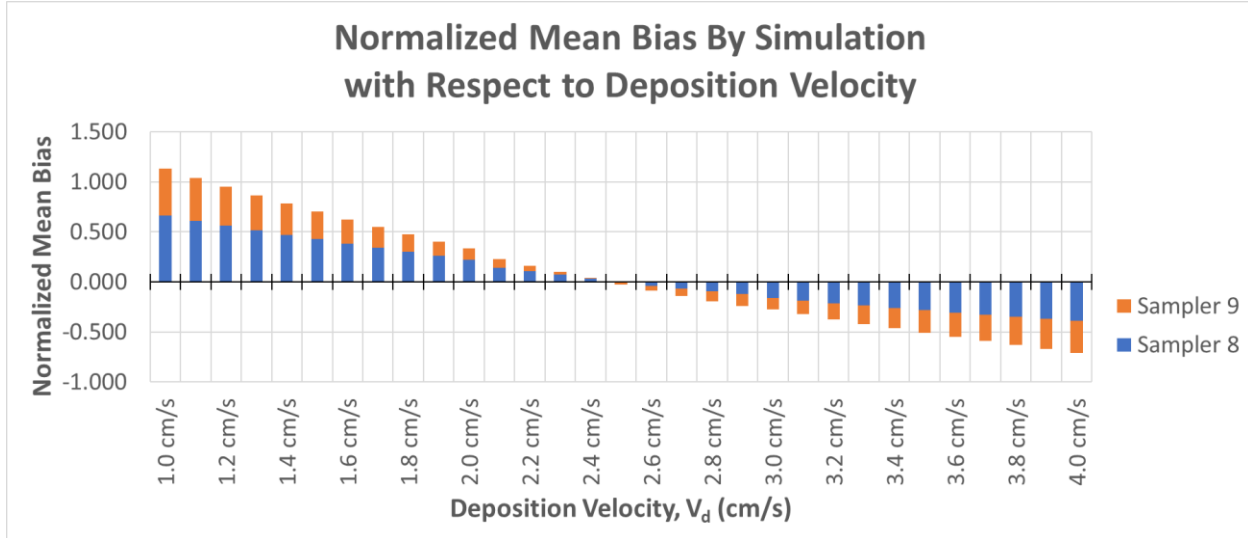


Figure 9. Normalized Mean Bias over all deposition velocities considered during the sensitivity analysis portion of the study. Sampler 8 and sampler 9 were the only samplers considered in the mean bias calculation due to other sampler's large error. Positive y-values indicate an overprediction of ammonia/nitrogen by the model while negative numbers indicate an underprediction by the model. The smaller the error, the better the results and a lack of bias in the model.

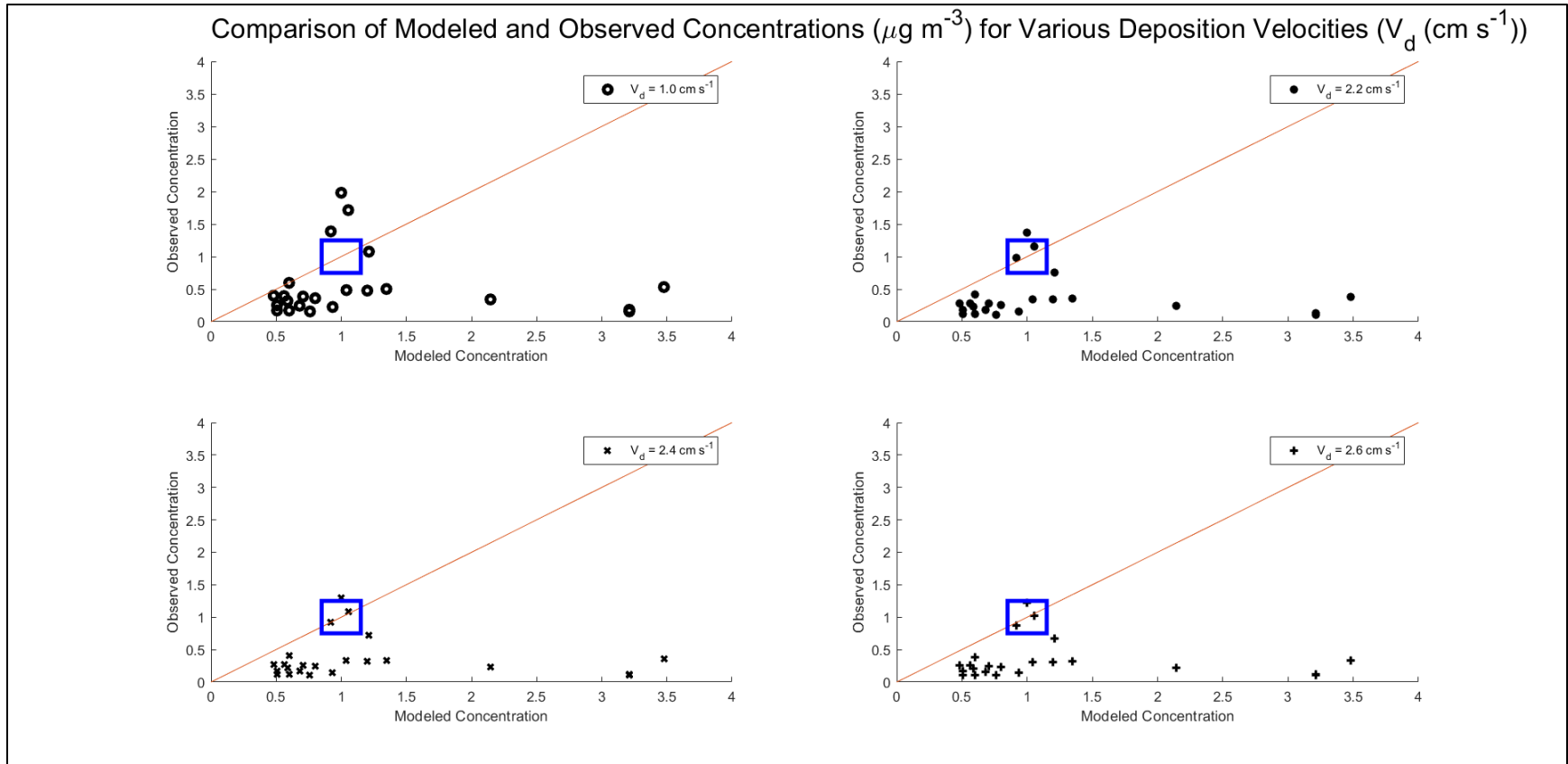


Figure 10. Comparison of modeled concentration against observed concentrations in the sensitivity analysis. This plot includes all samplers in the model as well as the modeled concentration based on select deposition velocities. The 1:1 ratio line is plotted in red to provide the line of best correlation. The blue box represents our area of interest and is the same for each graph.

Predominant Wind Speed & Direction for Salisbury, MD (KSBY)

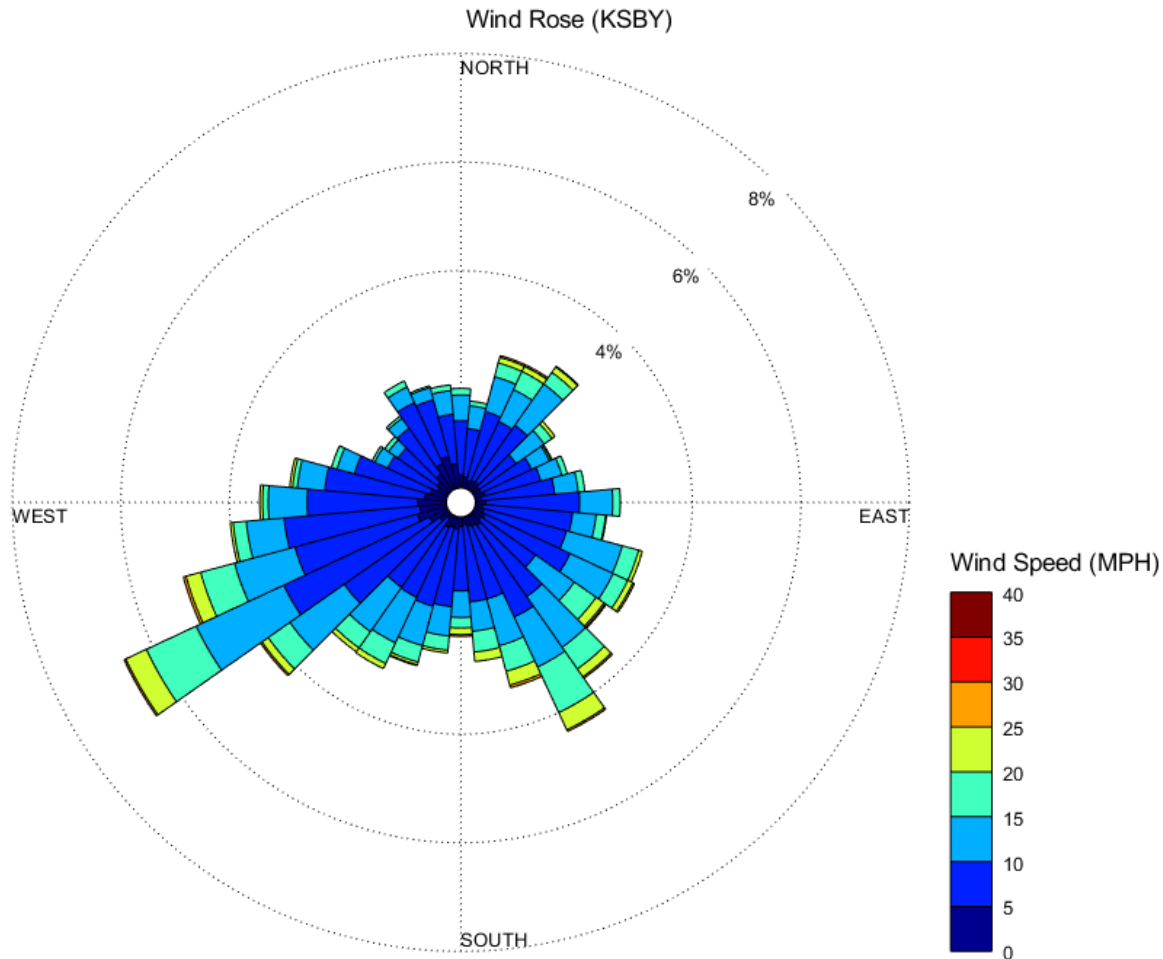


Figure 11. Wind rose for meteorology data used in all simulations associated with this study. The wind rose shows predominant wind speed and wind direction. Wind direction is noted by the spokes extending from the center of the wind rose. Wind speed is noted by the colors associated with each spoke in miles per hour (mph). Meteorology data is from Salisbury-Ocean City regional airport (KSBY) during 2017.

Total Ammonia/Nitrogen Deposition as a Function of Distance from the Source

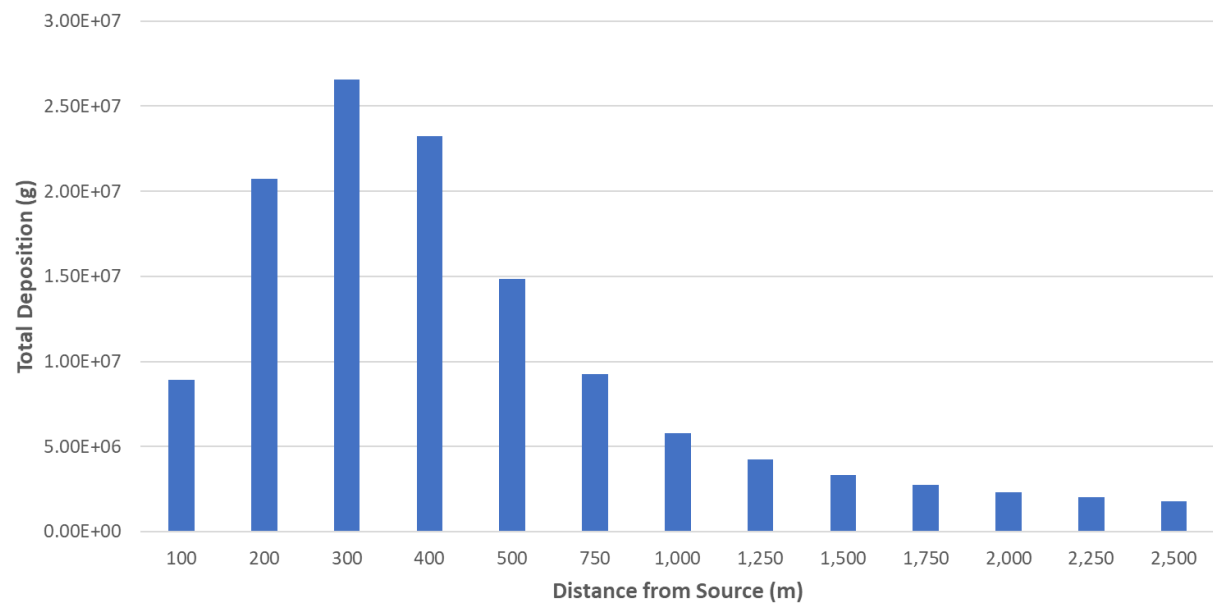


Figure 12. Total deposition of ammonia/nitrogen as a function of distance from a source (for a deposition velocity 2.4 cm/s), for a single poultry facility. On the y-axis, total deposition is indicated in units of grams. On the x-axis is distance from source in units of meters. A maximum of deposition is seen at 300 meters from the source.

Average Ammonia/Nitrogen Deposition Flux as a Function of Distance from Source

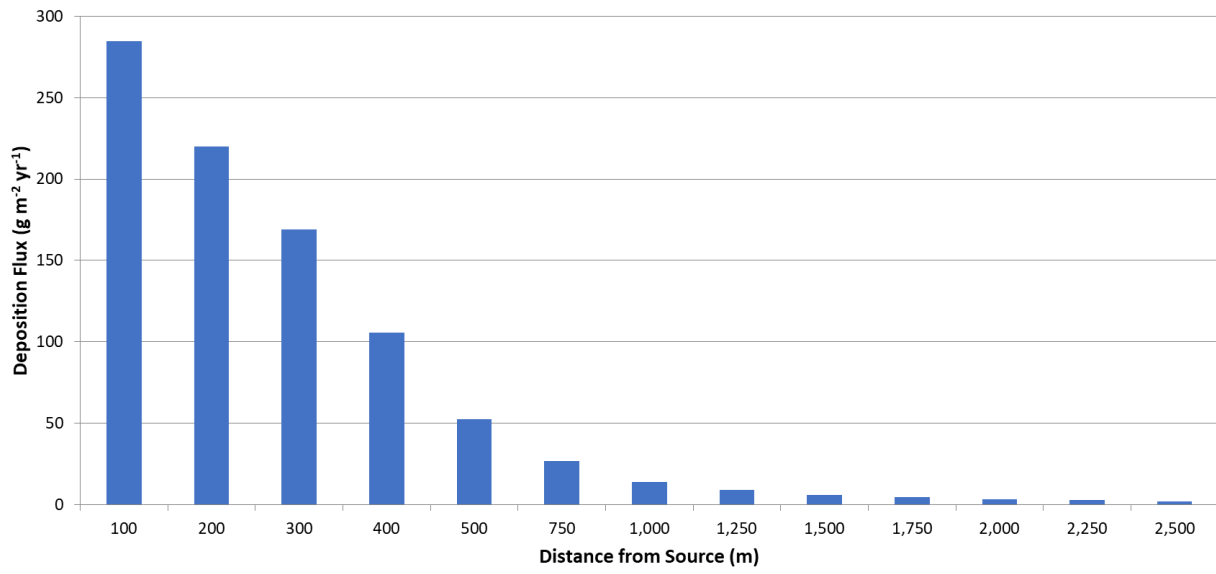


Figure 13. Average Annual Deposition Flux as a Function of Distance from an AFO source (for a deposition velocity of 2.4 cm/s), for a single poultry facility. A maximum of deposition flux occurs at the source with an exponential decrease away from the source location. At a distance of 2,500 m from the source, deposition flux becomes $2.8 \text{ g m}^{-2} \text{ yr}^{-1}$ and approaches 0 with little deposition occurring beyond 2,500 m away from the source.

Average Annual Ammonia Concentration

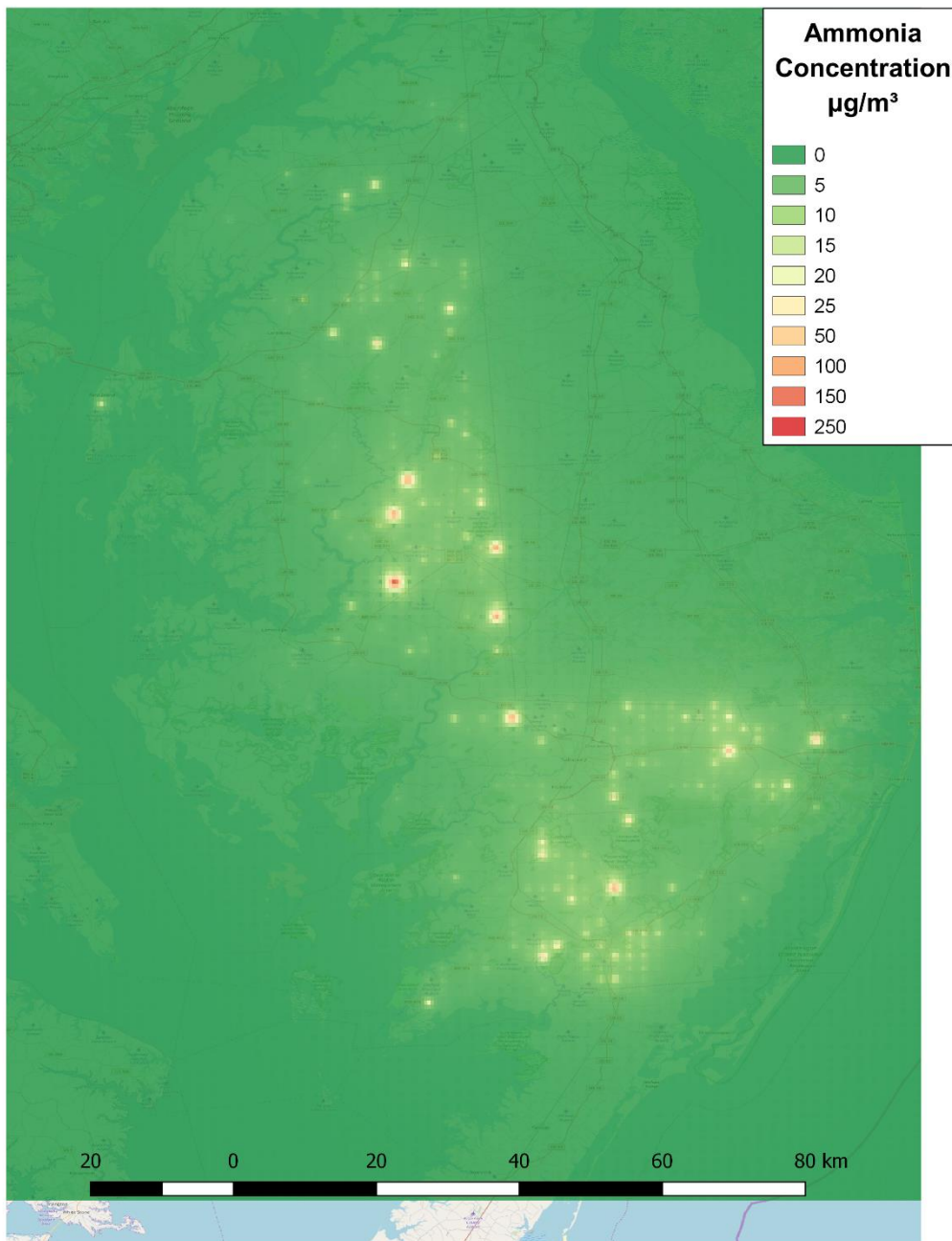


Figure 14. Average ammonia/nitrogen concentration over the Delmarva Peninsula during the 2017 year. The maximum of ammonia/nitrogen concentration at this time is $239 \mu\text{g m}^{-3}$. Concentration is calculated using a deposition velocity of 0.15cm/s .

Total Deposition Flux

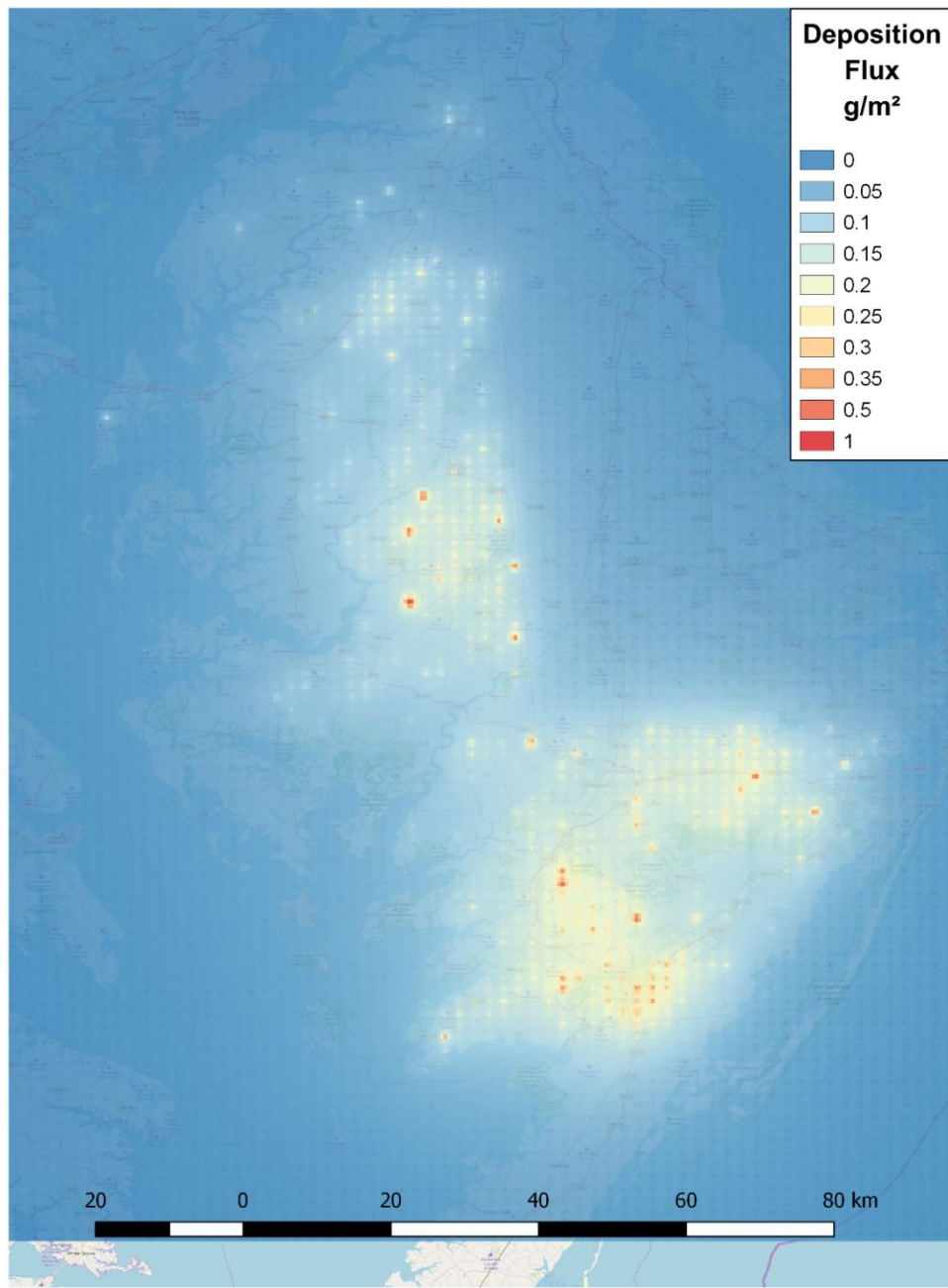


Figure 15. Annual deposition of ammonia/nitrogen including both dry and wet forms of ammonia/nitrogen. Units of the deposition results are in grams per meter squared. Most areas where deposition fluxes are greater than 0.5 g m^{-2} , are areas where CAFOs are located and a receptor is located in close proximity to the source. Deposition is calculated using a deposition velocity of 0.15 cm/s .

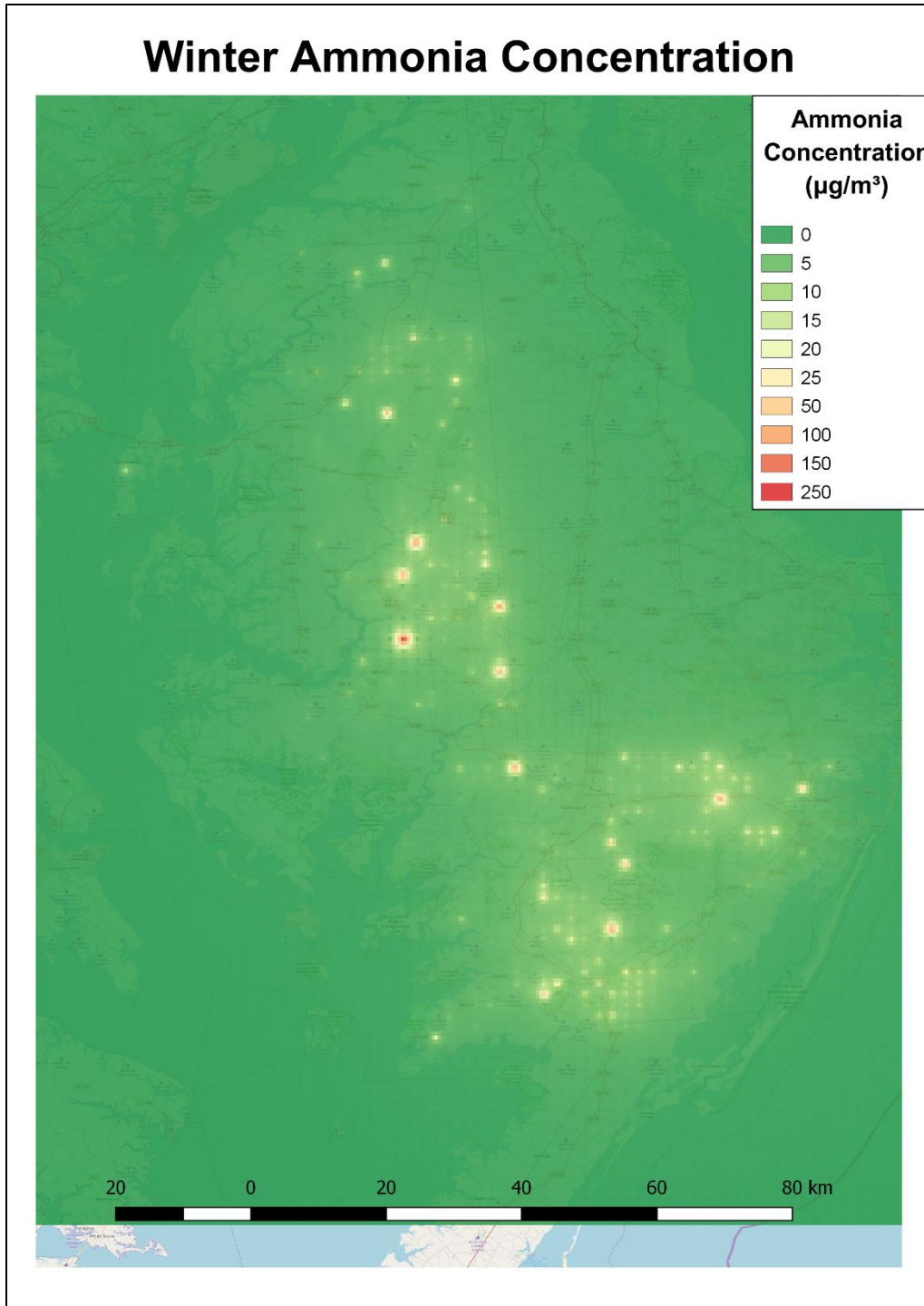


Figure 16. Average ammonia/nitrogen concentration over the Delmarva Peninsula during the winter. The maximum of ammonia/nitrogen concentration at this time is $267 \mu\text{g m}^{-3}$ which makes this the highest average ammonia/nitrogen concentration throughout the year. Calculated with a deposition velocity of 0.15 cm/s .

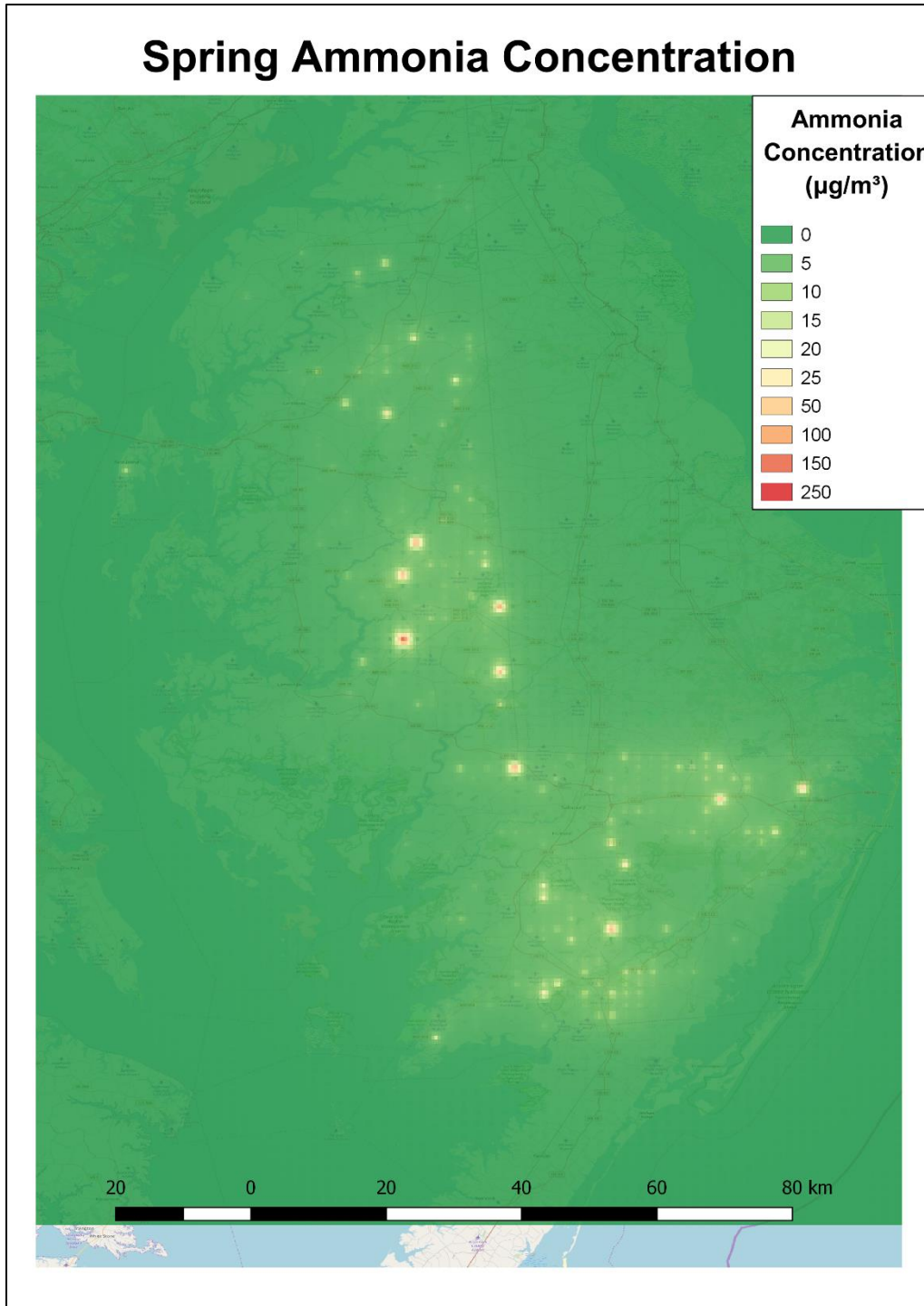


Figure 17. Average ammonia/nitrogen concentration over the Delmarva Peninsula during the spring season. The maximum of ammonia/nitrogen concentration at this time is $199 \mu\text{g m}^{-3}$ which makes this the lowest average ammonia/nitrogen concentration throughout the year. Calculated with a deposition velocity of 0.15 cm/s.

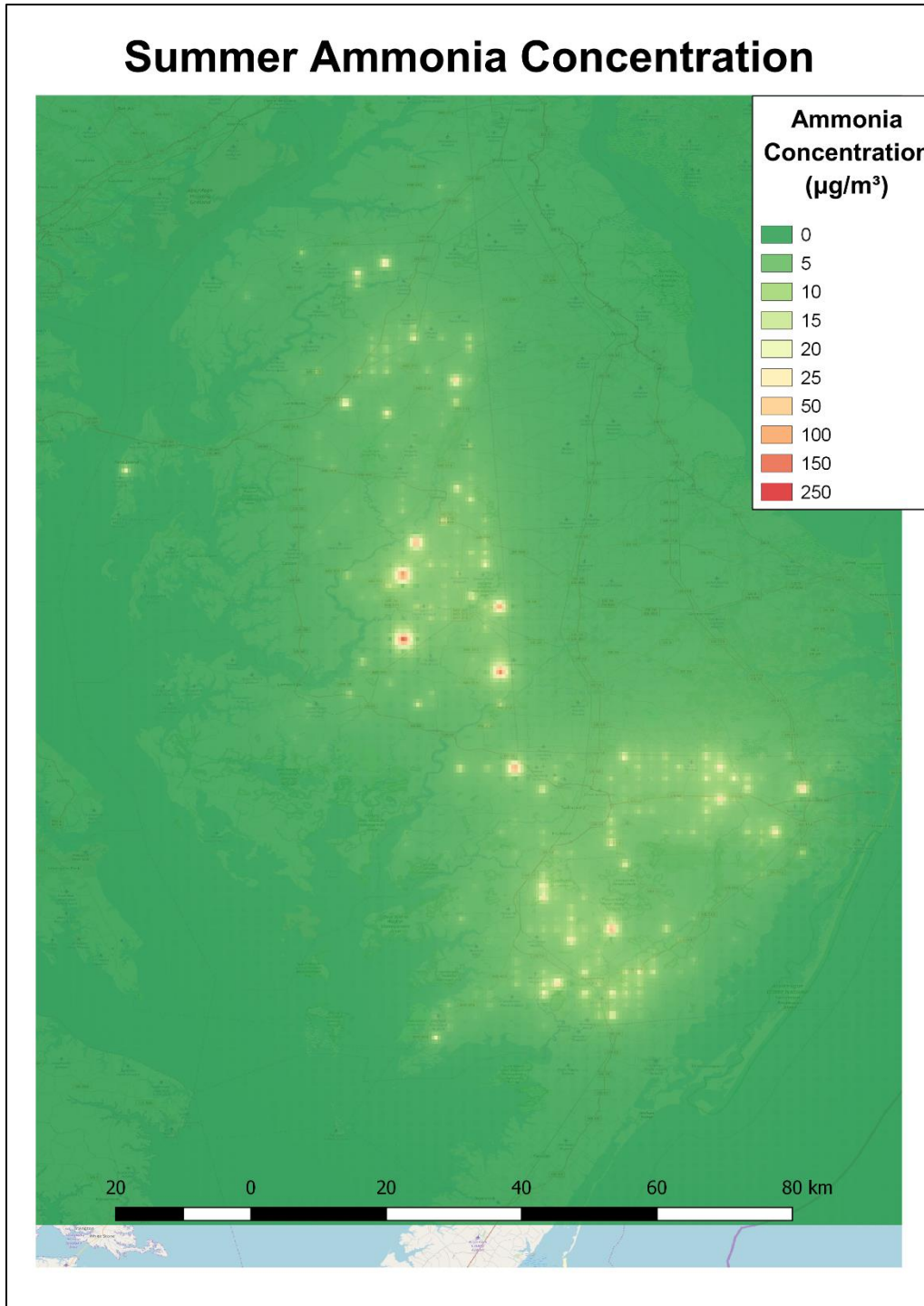


Figure 18. Average ammonia/nitrogen concentration over the Delmarva Peninsula during the summer season. The maximum of ammonia/nitrogen concentration at this time is $236 \mu\text{g m}^{-3}$ which makes this the third highest average ammonia/nitrogen concentration throughout the year. Calculated with a deposition velocity of 0.15 cm/s .

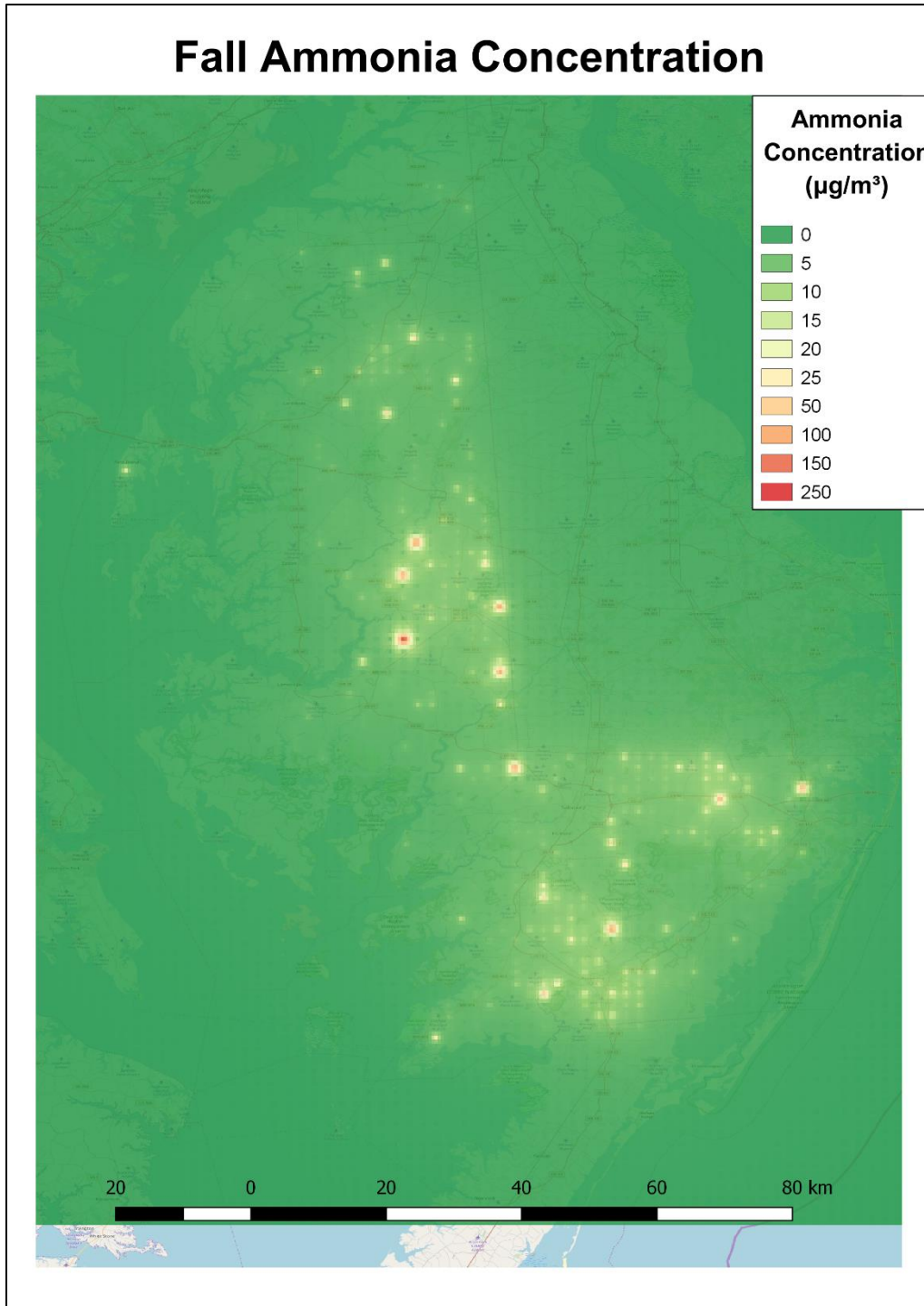


Figure 19. Average ammonia/nitrogen concentration over the Delmarva Peninsula during the fall season. The maximum of ammonia/nitrogen concentration at this time is $254 \mu\text{g m}^{-3}$ which makes this the second highest average ammonia/nitrogen concentration throughout the year. Calculated with a deposition velocity of 0.15 cm/s .

APPENDICES

Appendix A: Abstracts & Presentations

A-1: NC BREATHE 2017 Conference - Poster Abstract and Poster

Agricultural Ammonia/nitrogen Emissions on the Delmarva Peninsula: Transport and Deposition from a Poultry Concentrated Animal Feeding Operation

Jordan Baker*, Viney P. Aneja, and S. S. Pal Arya

North Carolina State University, Raleigh, NC 27695

*Corresponding Author:

(919) 515-3690 Telephone

(919) 513-8814 Fax

jlbaker4@ncsu.edu

Anthropogenic ammonia/nitrogen emission, especially from animal agriculture (i.e. concentrated animal feeding operations (CAFOs)) has become a major issue on the Delmarva Peninsula. The primary concern is deposition of nitrogen into tributaries that filter into the Chesapeake Bay leading to over enrichment and eutrophication of the ecosystem. In this area, excess nitrogen deposition from ammonia/nitrogen creates large algal blooms that deplete oxygen from the water. This study seeks to analyze ammonia/nitrogen transport and deposition in the vicinity of a poultry-producing CAFO. Employing the EPA-developed air quality dispersion model, AERMOD, the study examines transport and deposition around a representative poultry CAFO in Wicomico County, MD for 2012. On average, the highest ammonia/nitrogen concentrations occur during the summer. However some of the highest ammonia/nitrogen concentrations occur during the winter months within 50 m of the CAFO housing facility. An overall hourly-maximum ammonia/nitrogen concentration $5,905 \mu\text{g m}^{-3}$ (7.874 ppm) is calculated in the month of December during the morning hours. It is believed that these high concentrations are due to shallow boundary layer conditions or thermal inversions in the lower troposphere. Deposition is also calculated in the simulation using a deposition velocity for ammonia/nitrogen of 1.0 cm s^{-1} for agricultural sites. The simulation finds that total nitrogen deposition from a single CAFO is $15.1 \text{ kg NH}_3\text{-N per year}$. There is evidence that a single poultry facility can have a large effect on both the environment and nearby residents. Further model simulations suggest an inclusion of the bi-directional ammonia/nitrogen flux.

for presentation at:

2017 NC BREATHE Conference

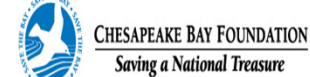
Tuesday, March 28, 2017

NC Museum of Natural Sciences, Raleigh, NC



Department of Marine, Earth &
Atmospheric Sciences

Agricultural Ammonia Emissions on the Delmarva Peninsula: Transport and Deposition from a Broiler Concentrated Animal Feeding Operation



Jordan Baker* (jlbaker4@ncsu.edu), Viney P. Aneja (vpaneja@ncsu.edu), and S. Pal Arya (sparya@ncsu.edu)

North Carolina State University, Raleigh, NC 27695-8208

Introduction

- Delmarva Peninsula has added hundreds of new poultry farms over the past decade
- The current air quality regulations have not compensated for the new addition of poultry operations on the Delmarva Peninsula and most facilities have been allowed to expand without any understanding of consequence to human health or to the Chesapeake Bay environment
- Ammonia (NH_3) is a very alkaline gas that greatly influences the pH of precipitation
- Ammonia reacts very quickly within the atmosphere (lifetime of hours to a couple of days) especially with liquid water.

Objective: To study the effects of a single broiler CAFO on the Delmarva Peninsula in an attempt to understand the impacts on humans and the local environment.



Figure 1. Average number of broilers and other poultry types per 100 acres. This figure shows the population density of broilers on the Delmarva Peninsula. The Delmarva Peninsula is one of the largest producers of poultry in the United States. The environmental effects from poultry production are scarcely studied despite a high population density leading to environmental and health problems for residents in the region.

Methods

- AERMOD, 2-D Gaussian Plume Model for simulating atmospheric dispersion
- Calculates dry and wet deposition as well as precipitation scavenging from meteorology data
- Concentration is calculated using the Gaussian model framework
- Meteorology is used from NWS Co-Op station 5 miles from the site with micrometeorological data calculated by the AERMET pre-processor
- The facility is treated as 4 separate area sources with animal waste being the primary pollutant. Broilers are the only type of animal housed by the facility.
- Emission factor is a combination of confinement, land application, and storage factors from Carnegie-Melon University. The total factor is 16.54 g $\text{NH}_3 \text{ bird}^{-1} \text{ month}^{-1}$

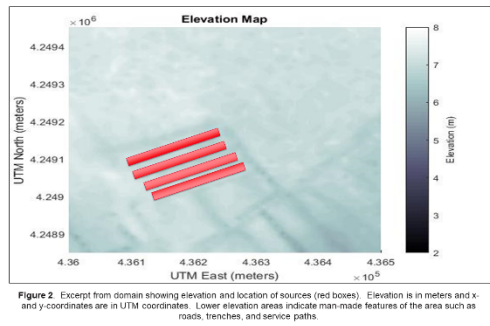


Figure 2. Excerpt from domain showing elevation and location of source (red boxes). Elevation is in meters and x- and y-coordinates are in UTM coordinates. Lower elevation areas indicate man-made features of the area such as roads, trenches, and service paths.

Results

Concentration Results

- Dispersion of pollutants with concentration above $100 \mu\text{g m}^{-3}$ occur at a maximum of approximately 400 meters from the center of the source cluster.
- Maximum concentrations are only present at the source, but concentrations $>150 \mu\text{g m}^{-3}$ are estimated by the model within 300 meters from the source.
- The maximum value of average concentration not occurring over the source region is $234.1 \mu\text{g m}^{-3}$ at a distance of 60 meters NW of the source.

Deposition Results

- Deposition in the form of wet ammonium (NH_4^+) occurs across most of the domain indicating that wet deposition can affect a very large area.
- Dry deposition contributes a much larger portion of the total deposition, but dry deposition is limited to areas near the source due to dispersion by the wind.
- Maximum of total deposition is $112.4 \text{ g m}^{-2} \text{ day}^{-1}$ only 20 meters north of the source region.
- Scavenging of ammonia by precipitation may have limited total deposition in the area.

Seasonal / Diurnal Results

- Receptors attained their maximum value in the early morning and just after sunset.
- Majority of the receptors attained a maximum value at 5 AM with daily thermal inversions caused by sensible heat fluxes becoming negative after sunset and the inversion deepening overnight.
- Winter and summer had the highest number of receptors reaching their maximum value with July and August being the month where most receptors reached their maximum.

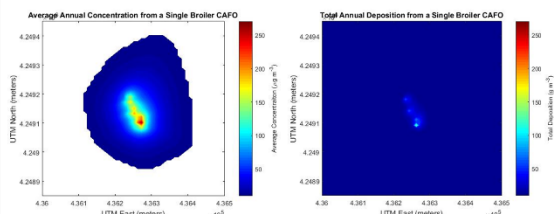


Figure 3. Average annual concentration of ammonia around the area sources defined in AERMOD, denoted as the farm listed in the simulation. This shows the concentration on average over the course of a year (2016) around the facility source. Coordinates are in UTM and are a small section of the total domain.

Figure 4. Total deposition including dry and wet deposition with effects of precipitation scavenging included. The image shows deposition occurring at all locations around the facility being considered. The domain shown in this image is that same as in Figure 3.



Figure 5. Maximum concentration at each receptor (model data point) listed in the AERMOD output and correlated with month of year in the graph on the right and correlated with time of day. Displayed is the number of receptors whose maximum value occurred at a given month of year (right) and hour of the day (left).



Conclusions

- Concentration downwind of the facility is dependent strongly on wind direction and wind speed.
- Temperature also has a strong effect on average concentration and deposition.
- Atmospheric stability is directly related to concentration maximums.
- Concentration maximums occur with atmospheric inversions.
- Diurnal inversions lead to concentration maximums and can be predicted based on this.
- Seasonal maximums are a function of atmospheric stability and temperature
 - High temperatures lead to higher emissions due to reaction rates.
 - Climatologically, winter is associated with stronger thermal inversions leading to concentration maximums.

- Wind direction is the principle factor in determining where the highest concentration will likely occur.
- Wind speed determines how far downwind pollutants will be dispersed.

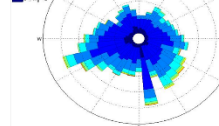


Figure 6. Wind speed and wind direction data from Co-Op site at Blackwater National Wildlife Refuge in Bucktown, Maryland. Each pie sector is represented in terms of frequency of a given wind direction with colors indicating sustained wind speed intensity.

Acknowledgements

I would like to thank Dr. James Thurman, Dr. Steven Perry, and Dr. John Walker at the US EPA for help with AERMOD Model Formulations, modeling setups, and modeling framework. An additional mention should be included for the USDA NASS Activity Data and Carnegie-Melon University for providing data on emissions from poultry facilities. Thank you to the State of Maryland Department of the Environment for CAFO data included in this study. Finally, I would like to acknowledge the Chesapeake Bay Foundation for their ongoing discussions and financial support as the scientific research continues.

References

- Anela, V. et al. (2008). Modeling Studies of Ammonia Dispersion and Dry Deposition at Some Hog Farms in North Carolina. *Journal of the Air & Waste Management Association*, 58(9), 1198–1207. doi:10.3155/1047-289X.58.9.1198
- ApSimon, H., M. Kruse, and J. Bell (1987). Ammonia emissions and their role in acid deposition. *Atmospheric Environment*, 21(9), 1939–1946. doi:10.1016/0004-6981(87)90154-5
- Asman, W. A. H., M. A. Sutton, and J. K. Schipper (1998). Ammonia emission, atmospheric transport and deposition. *New Phytologist*, 131(27–48), doi:10.1046/j.1469-3513.1998.00180.x
- Cooley, W. M., and R. T. Trivail (1950). A statistical procedure for determining the best performing air quality simulation model. *Atmospheric Environment*. Part A: General Topics, 24(0), 2387–2395. doi:10.1016/0960-1686(00)90314-6
- Denmead, O. J., F. Freney, and J. Simpson (1976). A closed ammonia cycle within a plant canopy. *Soil Biology and Biochemistry*, 8(2), 151–161. doi:10.1016/0038-0704(76)90033-1
- Inyang, I. S. (2001). A superstructure approach for dispersion model evaluation. *Journal of the Air & Waste Management Association*, 64(3), 255–264. doi:10.1080/10632727.2013.833147
- Russell, K. M., J. N. Galloway, S. A. Macko, J. L. Moody, and J. R. Scularkorn (1998). Sources of nitrogen in wet deposition to the Chesapeake Bay region. *Atmospheric Environment*, 32(14–15), 2453–2465. doi:10.1016/S1364-2310(98)00044-2
- Scholes, J. A., and A. Lynn (2002). Modeling Atmospheric Nitrogen Deposition and Transport in the Choptank River Watershed. *Journal of Quality*, 31(4), 1194. doi:10.2134/jeq2002.1194
- Sutton, M. A., W. A. H. Asman, and J. K. Schipper (1994). Dry deposition of reduced nitrogen. *Tellus B*, 46(4), doi:10.3402/tellusb.v46.1579. *Environment*.

Can AERMOD Accurately Predict Ammonia/nitrogen Concentrations in Areas of Heavy Agricultural Production?

Jordan Baker*, Viney P. Aneja, and S. S. Pal Arya

North Carolina State University, Raleigh, NC 27695

*Corresponding Author:

(919) 515-3690 Telephone

(919) 513-8814 Fax

jlbaker4@ncsu.edu

Although ammonia/nitrogen is well understood, it is very difficult to model. The reason for this is that local sources of NH₃ are a significant determinant in the measured concentration at a given location. Most dispersion models tend to fall short in accurately representing ammonia/nitrogen concentration because they cannot capture these localized sources. However, if large sources of ammonia/nitrogen are near these localized sources, the smaller sources can be overwhelmed, increasing the predictability of ammonia/nitrogen concentrations. Mirroring Eastern North Carolina's hog industry, the Eastern Shore of Maryland is a national leader in poultry production and ammonia/nitrogen emissions. Using Maryland AFO data, all poultry operations on the Maryland Eastern Shore were modeled using the AERMOD dispersion model and treated as sources for computational analysis at 23 locations of interest. Meanwhile, samplers were placed for 28 days at these areas of interest to collect ground-based concentrations. A sensitivity analysis was conducted to find a realistic value of ammonia/nitrogen deposition velocity (cm/s), beginning with a value of 1.0 and iterating by 0.1 to a maximum of 4.0. A deposition velocity of 2.4 cm/s gives a percent difference of about 1% at two sampling locations in the center of the Delmarva Peninsula. These locations were surrounded by a large concentration of poultry CAFOs. Where monitoring sites are near urban and marine sources, ammonia/nitrogen concentrations are much different. Given these results, it is determined that AERMOD can accurately predict ammonia/nitrogen concentration in areas where prominent sources can be found. There is a significant decrease in the model's ability as you move away from the highest density of sources. However, understanding that AERMOD has the ability to predict model concentrations and deposition can help us determine how much ammonia/nitrogen these poultry CAFOs are contributing to their local environment, and in some cases, their region.

for presentation at:

2018 NC BREATHE Conference

Thursday, March 8, 2018

Wake Forest School of Medicine, Winston-Salem, NC



Department of Marine, Earth & Atmospheric Sciences

Can AERMOD Accurately Predict Ammonia Concentrations in Areas of Heavy Agricultural Production?

Jordan Baker* (jlbaker4@ncsu.edu), V. P. Aneja (vpaneja@ncsu.edu), W. P. Robarge (nwpr@ncsu.edu) and S. P. Arya (sparya@ncsu.edu)
North Carolina State University, Raleigh, NC 27695-8208

Introduction

- Delmarva Peninsula has added hundreds of new poultry farms over the past decade
- The current air quality regulations have not compensated for the new addition of poultry operations on the Delmarva Peninsula and most facilities have been allowed to expand without any understanding of consequence to human health or to the Chesapeake Bay environment
- Ammonia (NH_3) is a very alkaline gas that greatly influences the pH of precipitation
- Ammonia reacts very quickly within the atmosphere (lifetime of hours to a couple of days) especially reactive with liquid water.

Objective: To conduct a sensitivity analysis on the Maryland Eastern Shore in an attempt to predict ammonia concentrations in heavy broiler production areas.



Figure 1. Average number of broilers and other poultry types per 100 acres. This figure shows the population density of broilers on the Delmarva Peninsula. The Delmarva Peninsula is one of the largest producers of poultry in the United States. The environmental effects from poultry production are scarcely studied despite a high population density leading to environmental and health problems for residents in the region.

Methods

- AERMOD, 2-D Gaussian Plume Model for simulating atmospheric dispersion
- Calculates ammonia concentration, dry and wet deposition, as well as precipitation scavenging from meteorology data (provided from NOAA data network).
- Concentration is calculated using the Gaussian model framework (with similar meteorology) over the same time period as sampling campaign (Sept-Oct, 2017).
- Sampling data were collected over 2 trips for 14 days each (September through early October) with passive Alpha samplers at 23 locations.
- The facilities included are >600 broiler CAFOs on the Maryland Eastern Shore and are modeled with 23 sampler locations on the Eastern Shore of MD.
- Emission factor is a combination of confinement, land application, and storage factors from Carnegie-Melon University (2004). The total factor is 0.55 g $\text{NH}_3 \cdot \text{bird}^{-1} \cdot \text{day}^{-1}$

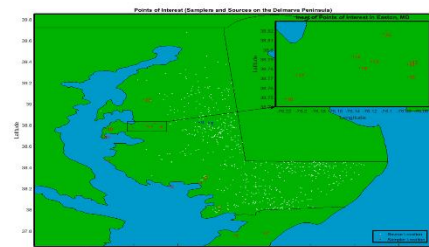


Figure 2. Excerpt of Maryland Eastern Shore and domain used in the AERMOD model showing location of sources (white dots) and sampler locations (red blocks). Numbers indicate the sampler number used in passive sampler analysis. Blue text and blue boxes show areas where sensitivity analysis was heavily influenced by CAFO operations.

Results

Passive Sampling Results (23 Locations)

- Sampler results on the second trip were limited due to meteorological conditions.
- Maximum concentrations were measured in an urban area and not in the agricultural center as expected. This is likely due to the localized sources associated with urban and marine locations.
- Sampler 8 and sampler 9 are located in the center of a heavy agricultural area and are used as the main focal point of our sensitivity analysis because measured concentrations at sampler 8 and 9 are likely influenced by CAFOs and other agricultural sources.

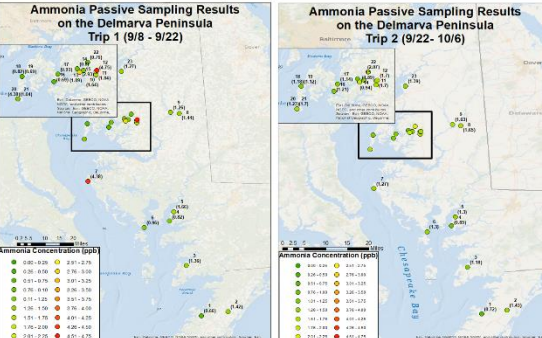


Figure 3. Sampling results from the first trip of placing passive samplers. This trip occurred from September 8 to September 22 and ALPHAs samplers were placed at 23 locations and accurately modeled using AERMOD. Concentrations on this trip were much higher than those of the second trip.

Figure 4. Sampling results from the second trip of placing passive samplers. This trip occurred from September 22 to October 6 and ALPHAs samplers placed at 23 locations were accurately modeled using AERMOD. Concentrations on this trip were analyzed. Concentrations on this trip were much lower than those of the first trip.

Modeling Results over Same Period

- Deposition velocities from 1.5 cm/s to 3.5 cm/s were considered, but results for 2.1 cm/s to 2.7 cm/s are shown. This is derived from literature suggestions. Deposition velocities are an average over a day and do not include diurnal variations.
- Dry deposition contributes a much larger portion of the total deposition, but dry deposition is limited to areas near the source due to dispersion by the wind.
- Minimum absolute error is found at 2.4 cm/s with an error of only 0.8%.

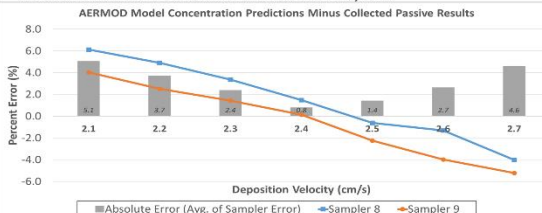


Figure 5. Difference of AERMOD Model predictions and actual passive sampler data. Sampler 8 and Sampler 9 were the only samplers considered in this analysis because of local sources. Absolute error is the average of the percent difference between sampler 8 and sampler 9. Due to these results, the best selection for deposition velocity was 2.4 cm/s. This is confirmed by Phillips et al. (2004).



Department of Marine, Earth & Atmospheric Sciences

Conclusions

- A deposition velocity of 2.4 cm/s gives accurate concentration predictions within 0.8%. This small percent difference proves that AERMOD can accurately predict ammonia concentrations especially in areas of heavy agricultural production.
- Samplers away from CAFOs and agricultural sources have very high concentration readings which is likely due to urban and marine sources.

$$\text{Deposition Flux} = \text{Concentration} \times \text{Vd}$$

- According to concentration results as well as deposition formulations within the AERMOD model, being able to accurately predict concentrations will also lead to accurate predictions of deposition flux and total dry deposition.

Limitations

- Bi-directional flux was not included in this simulation and could be a point of limitation for the data along with a lack of vertical distribution of ammonia.
- Deposition velocities were fixed throughout the simulation and ideally, varying the velocities based on atmospheric conditions would be more accurate.
- Not all agricultural sources are modeled in the AERMOD calculation. CAFOs are considered in the calculation without synthetic fertilizer included.

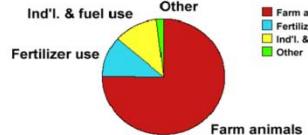


Figure 6. Distribution of ammonia emission sources in the United States using 1996 NASS data. Emissions have not changed much since 1996. This research was presented by William Arya of NC State University in preparation for NOAA Air Resources Laboratory and the EPA Chesapeake Bay Program in 2000.

Acknowledgements

I would like to thank Dr. James Thurman, Dr. Steven Perry, and Dr. John Walker at the US EPA for help with AERMOD Model Formulations, modeling setups, and modeling framework. An additional mention should be included for the USDA NASS Activity Data and Carnegie-Melon University for providing data on emissions from poultry facilities. Thank you to the State of Maryland Department of the Environment for CAFO data included in this study. Finally, I would like to acknowledge the Chesapeake Bay Foundation for their ongoing discussions and financial support as the scientific research continues.

References

- Aneja, V. et al. (2008). Modeling Studies of Ammonia Dispersion and Dry Deposition at Some Hog Farms in North Carolina. *Journal of the Air & Waste Management Association*, 58(9), 1198–1207. doi:10.3155/1047-3289.58.9.1198.
- ApSimon, H., M. Kruse, and J. Bell (1987). Ammonia emissions and their role in acid deposition. *Atmospheric Environment*, 21(19), 1939–1944. doi:10.1016/0004-6981(87)90154-5.
- Asman, W. A. H., M. A. Sutton, and J. K. Schorrung (1998). Ammonia: emission, atmospheric transport and deposition. *Atmospheric Environment*, 32(12), 245–264. doi:10.1016/S0004-6981(98)00160-1.
- Cox, W. M., and J. A. Tivatt (1990). A statistical procedure for determining the best performing air quality simulation model. *Atmospheric Environment*, Part A: General Topics, 24(9), 2387–2395. doi:10.1016/0960-1686(90)90331-q.
- Denmead, O., J. Freney, and J. Simpson (1976). A closed ammonia cycle within a plant canopy. *Soil Biology and Biochemistry*, 8(2), 161–164. doi:10.1016/0038-0706(76)90014-9.
- Horn, R. C. (1994). A suggested ammonia dispersion model evaluation. *Journal of the Air & Waste Management Association*, 64(3), 255–264. doi:10.1080/10862247.2013.833147.
- Russell, K. M., J. N. Galloway, S. A. Macko, J. L. Moody, and J. R. Scudark (1998). Sources of nitrogen in wet deposition to the Chesapeake Bay region. *Atmospheric Environment*, 32(14–15), 2433–2465. doi:10.1016/S1352-2310(98)00044-2.
- Scholes, D. J., and J. A. Tivatt (2002). Modeling Atmospheric Nitrogen Deposition and Transport in the Chesapeake Bay Watershed. *Journal of Quality*, 31(4), 1194. doi:10.2134/jeq2002.1194.
- Sutton, M., A. W. H. Asman, and J. K. Schorrung (1994). Dry deposition of reduced nitrogen. *Tellus B*, 46(4), doi:10.3402/tellusb.v46.15796. *Environment*.